U.S. Army Medical Research
Institute of Chemical Defense

USAMRICD-TR-06-08

Bioanalytical Method to Determine the Effects of Cyanide, Cyanide Metabolites and Cyanide Antidotes on the Activity of Cytochrome C Oxidase Immobilized in an Electrode Supported Lipid Bilayer Membrane

James B. Kelly
Steven I. Baskin

June 2006

U.S. Army Medical Research
Institute of Chemical Defense
Aberdeen Proving Ground, MD 21010-5400

DISPOSITION INSTRUCTIONS:

Destroy this report when no longer needed. Do not return to the originator.

DISCLAIMERS:

The opinions or assertions contained herein are the private views of the author(s) and are not to be construed as official or as reflecting the views of the Army or the Department of Defense.

The use of trade names does not constitute an official endorsement or approval of the use of such commercial hardware or software. This document may not be cited for purposes of advertisement.

REPORT DOCUMENTATION PAGE

Form Approved
OMB No. 0704-0188

1. REPORT DATE *(DD-MM-YYYY)*	2. REPORT TYPE	3. DATES COVERED *(From - To)*
June 2006	Technical Report	September 2005 - December 2005

4. TITLE AND SUBTITLE
Bioanalytical Method to Determine the Effects of Cyanide, Cyanide Metabolites and Cyanide Antidotes on the Activity of Cytochrome C Oxidase Immobilized in an Electrode Supported Lipid Bilayer Membrane

5a. CONTRACT NUMBER

5b. GRANT NUMBER

5c. PROGRAM ELEMENT NUMBER
61101A

6. AUTHOR(S)
Kelly, J.B., Baskin, S.I.

5d. PROJECT NUMBER
91C

5e. TASK NUMBER

5f. WORK UNIT NUMBER

7. PERFORMING ORGANIZATION NAME(S) AND ADDRESS(ES)

US Army Medical Research Institute of Chemical Defense
ATTN: MCMR-CDT-N
3100 Ricketts Point Road
Aberdeen Proving Ground, MD 21010-5400

8. PERFORMING ORGANIZATION REPORT NUMBER
USAMRICD-TR-06-08

9. SPONSORING / MONITORING AGENCY NAME(S) AND ADDRESS(ES)

US Army Medical Research Institute of Chemical Defense
ATTN: MCMR-CDA-T
3100 Ricketts Point Road
Aberdeen Proving Ground, MD 21010-5400

10. SPONSOR/MONITOR'S ACRONYM(S)

11. SPONSOR/MONITOR'S REPORT NUMBER(S)

12. DISTRIBUTION / AVAILABILITY STATEMENT

Approved for public release; distribution unlimited

13. SUPPLEMENTARY NOTES

14. ABSTRACT
The bioanalytical studies pursued in this research take advantage of the electron transfer reactivity of cytochrome c oxidase (CCO) when immobilized in a bilayer attached to an electrode surface. This enzyme immobilization method enables CCO to exhibit reaction chemistry that mimics its *in vivo* behavior because the bilayer structure is thought to reproduce its *in vivo* environment in the inner mitochondrial membrane.[1-8] In addition this experimental platform for CCO enables an innovative and direct screening assay for toxic substances and potential antidotes for inhibition of this enzyme by these substances. The preliminary results obtained thus far describe the following:

1) An alternate programmable reference oscillator that is compatible with the electronic circuitry in the quartz crystal microbalance obtained from CH Instruments.
2) Octadecyl mercaptan deposition control.
3) Possibility for chloride interference in the potential window of the experiment.
4) Additional analytical methods to supplement electrochemical results obtained.
    a. Spectroelectrochemistry experimental design.
    b. New bioanalytical method for detecting cyanide using metmyoglobin.

15. SUBJECT TERMS
Spectroelectrochemistry, biosensor, electrode, cytochrome c oxidase, metmyoglobin, cyanide, metabolites, antidotes, therapies

16. SECURITY CLASSIFICATION OF:			17. LIMITATION OF ABSTRACT	18. NUMBER OF PAGES	19a. NAME OF RESPONSIBLE PERSON
a. REPORT	b. ABSTRACT	c. THIS PAGE			James B. Kelly
UNCLASSIFIED	UNCLASSIFIED	UNCLASSIFIED	UNLIMITED	37	19b. TELEPHONE NUMBER *(include area code)* 410-436-2055

Acknowledgements:

Special thanks for Dr. Fred Hawkridge at Virginia Commonwealth of Virginia and Dr. Ed Bowden at North Carolina State University for their advice, comments and the large supply of cytochrome c oxidase. Their extensive experience (> 30 years) and knowledge in the area of electrochemistry of enzymes and proteins could easily overwhelm anyone, but their advice and explanations always proved helpful and will give confidence to even the novice in this area.

The authors would also like to thank all the colleagues at the Medical Research Institute of Chemical Defense (ICD) for their support and funding of this work. Especially the prior commander, COL Gennady Platoff, the protocol reviewers, Dr. Tom Logan and Dr. Ben Capacio, Dr. Gary Rockwood, who is the cyanide research coordinator, and the branch chief at the time, CPT Matthew Clark.

Summary:

The bioanalytical studies pursued in this research take advantage of the electron transfer reactivity of cytochrome c oxidase (CCO) when immobilized in a bilayer attached to an electrode surface. This enzyme immobilization method enables CCO to exhibit reaction chemistry that mimics its *in vivo* behavior because the bilayer structure is thought to reproduce its *in vivo* environment in the inner mitochondrial membrane.[1-8] In addition this experimental platform for CCO enables an innovative and direct screening assay for toxic substances and potential antidotes for inhibition of this enzyme by these substances.

The goals of this research are to:

1) Continue to examine the viability of the modified CCO electrode as a unique biosensor.
2) Compare the toxicity of cyanide and cyanide metabolites towards CCO and to kinetically compare the function of antidotes.
    a. Supplement electrochemical results obtained by developing or establishing additional analytical methods for the detection of free cyanide and cyanide that is bound to CCO.

The preliminary results obtained thus far describe the following:

1) An alternate programmable reference oscillator that is compatible with the electronic circuitry in the quartz crystal microbalance obtained from CH Instruments.
2) Octadecyl mercaptan deposition control.
3) Possibility for chloride interference in the potential window of the experiment.
4) Additional analytical methods to supplement electrochemical results obtained.
    a. Spectroelectrochemistry experimental design.
    b. New bioanalytical method for detecting cyanide using metmyoglobin.

Table of Contents: **Page**

I. Introduction:

a. Cyanide history

Historically, cyanide has been used by military and terror groups as a weapon, and it has also been responsible for injuries and deaths in civilian experiences such as fires, poisonings and industrial accidents.[9] From as early as the Roman Empire to present day cyanide has killed millions of people. Cyanide compounds are easily accessible commercially due to the many industrial processes that use it or dispose of it as a byproduct. Even though there are less volatile or more persistent chemical agents on the large scale battlefield, there are many situations in which soldiers are in closed spaces, such as combat support hospitals, dining halls, gyms, etc., where cyanide compounds, used by rogue terror groups, could quickly deliver lethal effects. While some terror groups may consider cyanide less useful due to its volatility, others may find it more attractive since troops may enter the area without protective gear soon after an attack and the detection of cyanide is often more difficult, especially in hot climates.

b. CCO description

Cytochrome c oxidase is the terminal enzyme in the mitochondrial oxidative phosphorylation chain and a crucial enzyme for aerobic respiration.[10] The catalytic core of bovine CCO is composed of subunits I, II and III, and they are mitochondrially encoded.[11] Bovine CCO redox activity stems from four redox centers that reside in subunits I and II: two iron centers, heme *a* and heme a_3, and two copper centers, Cu_A and Cu_B. Subunit I contains three of these redox centers: the low spin heme *a* and the high spin heme a_3 - Cu_B (the dioxygen binding site). Subunit II of CCO, located on the cytosolic side, contains the binuclear Cu_A center, receives its electrons from solution resident cytochrome *c* via binding to the subunit II and transfers the electrons to heme *a* and finally to the dioxygen binding site.[12, 13]

$$\text{Cytochrome } c^{2+} \rightarrow Cu_A \rightarrow \text{/heme } a \rightarrow \text{/heme } a_3/Cu_B \text{ site} \rightarrow O_2$$

Cytochrome c oxidase catalyzes the reduction of dioxygen to two waters via the following overall reaction:[7] $4\ \text{Cytochrome } c^{2+} + 4\ H^+ + O_2 \rightarrow 4\ \text{Cytochrome } c^{3+} + 2\ H_2O$.

This exergonic reaction liberates free energy that is used to pump protons across energy-transducing membranes, creating an electrochemical gradient that is used in the production of ATP.[14] The exact mechanism by which dioxygen is reduced to water and whether the mechanism is sequential or branched are not known.[15-18]

c. CCO and cyanide toxicity

It is believed that the primary reason for the toxicity of cyanide is the inhibition of CCO activity. Cyanide blocks CCO's ability to reduce oxygen to water, which terminates the production of adenosine triphosphate (ATP) at that step.[9, 19, 20] The high spin heme a_3/Cu_B in CCO is the redox center that is thought to be responsible for cyanide binding as well as for binding to a variety of other inhibitor ligands such as nitric oxide and carbon monoxide.[8, 10, 11, 14, 21-28] Many publications have addressed the inhibition of CCO by cyanide; however, there are still inconsistencies in the literature as to the exact mechanism. For example, whether there is proton dissociation upon

binding to the heme iron, leaving cyanide axially coordinated to the heme a_3 or bridged to Cu_B^{2+}, is problematic.[21-27]

There are other biochemical processes affected by cyanide,[9, 19, 20] and there is recent evidence that the cyanide metabolite 2-aminothiazoline-4-carboxylic acid (ATCA) is also toxic. ATCA is a minor cyanide metabolite that is formed by combination with free cystine during cyanide intoxification, and its metabolism increases as cyanide concentrations increase.[29] Production of ATCA is found predominately in organs of the body where rhodanese levels are low, such as the brain and heart, and has been found to be a neurotoxicant, forming hippocampal CA1 lesions in rodents.[30] Large amounts of CCO are also found in the heart; however, no published literature to date has thoroughly examined the effects, if any, of ATCA on CCO.

d. Cyanide antidotes

The cyanide antidotes used clinically in the treatment of CN intoxication can be divided into two groups. Group 1 antidotes increase the rhodanese sulfurtransferase reactions, and group 2 antidotes bind to cyanide to form a less toxic product.[31] The group 1 antidotes are sulfur donors that increase the activity of the sulfurtransferases, rhodanese and 3-mercaptopyruvate. The sulfurtransferases catalyze the transfer of a sulfane sulfur atom from a donor to the suitable sulfur acceptor, cyanide, to form the less toxic thiocyanate.[31-33]

$$\text{Donor-S-S} + CN^- \rightarrow \text{Donor-S} + SCN^-$$

Rhodanese, a mitochondrial sulfurtransferase, is thought to be the more important sulfurtransferase in cyanide intoxication as compared to 3-mercaptopyruvate sulfurtransferase due to its large concentrations, high turnover number and closer proximity to CCO in the mitochondria. There are various sources of donors, such as thiosulfate, thiosulfonates, serum albumin-sulfane complex, etc., but it is the sulfur donor thiosulfate that is in clinical use[31, 34] for treating cyanide poisoning. Several studies have also suggested that rhodanese can reactivate CCO inhibited by cyanide.[35-37] It should be mentioned that since thiosulfate does not quickly penetrate the mitochondrial membrane, thiosulfate is taken with other antidotes, and research groups continue to search for a more suitable sulfur donor.[33]

The group 2 antidotes (methemoglobin formers, hydroxycobolamin, cobalt EDTA) are scavengers for free cyanide, forming less toxic cyanide complexes; however, it has been suggested in the literature that some of them may also reactivate cyanide-inhibited CCO.[38-40] Methemoglobin formers are used to produce a condition called methemoglobinaemia, a condition in which there is a large concentration of oxidized hemoglobin (methemoglobin) in blood. Methemoglobin has a higher affinity for cyanide than hemoglobin and binds with cyanide to form cyanomethemoglobin. Amyl nitrite, sodium nitrite and 4-dimethylaminophenol (4-DMAP) are the most common clinically used methemoglobin formers in the treatment of cyanide poisoning. The cobalt compounds hydroxycobolamin and cobalt EDTA form a stable metal complex with cyanide and are also clinically used in the treatment of cyanide poisoning.[31, 40-48]

Whether the antidote is a sulfur donor for rhodanese or binds directly to cyanide, both cyanide antidote groups act to function as cyanide scavengers, and some have also been suggested to

reactivate cyanide-inhibited CCO.[35, 36, 38-40, 49] It is the antidotes' scavenging ability (protecting CCO from inhibition) and their ability to directly reactivate inhibited CCO that is to be investigated and compared. Even though there may be other chemical mechanisms that antidotes may experience after injection and before reaching their destination (cyanide contaminated mitochondria), this innovative assay can be used as a model for interactions with CCO and will help provide insight to animal work.

e. CCO modified electrodes

The experimental platform to be used is based on earlier work in which beef heart CCO was immobilized into an electrode supported lipid bilayer membrane (LBM).[1-8] Based on Hawkridge and coworkers' experimental results[1-8] this modified CCO electrode closely mimics the *in vivo* behavior of CCO and its *in vivo* environment in the inner mitochondrial membrane. It provides a structure of uniform distribution of enzyme orientations such that the oxygen reduction site faces the electrode surface and the oxidation site for cytochrome c protrudes into solution. The thin immobilization matrix has a membrane thickness of about 5 nm or 50 Å. This matrix maintains the enzyme in active form, protecting against thermal and chemical degradation and preventing enzyme leaching, and helps to eliminate problems caused by substrate/analyte diffusion through common immobilization matrices, usually about 1 μ or 10,000 Å thick. No other enzyme-modified electrode reported thus far in the literature has this structure.

To integrate CCO into a lipid bilayer onto an electrode surface one must also consider the type of electrode and any initial steps that might be necessary to prepare a favorable electrode surface. A procedure was developed by Hawkridge and coworkers that allowed electrode communication with the enzyme after several years of unsuccessful attempts to integrate CCO into lipid bilayers on electrodes using Langmuir-Blodgett techniques.[1, 3, 5] Initially this new procedure (led by Cullison) involved submonolayer coverages of octadecyl mercaptan (OM) on gold electrodes.[5] The octadecyl mercaptan (OM) molecule provides hydrophobic interactions with the hydrophobic regions of the lipids and CCO, resulting in a more stable bilayer membrane. In addition the submonolayer coverage will still allow access to the electrode for CCO during the dialysis step. Burgess later electrochemically deposited enough silver for monolayer coverage on the gold electrode before the OM self-assembly.[1] The silver deposit step led to an increase in reproducibility of the OM deposition and the lipid bilayer formation.[1, 3] This is attributed to the stronger silver-sulfur bond and to the OM orientation being normal to 15^{o} relative to the silver electrode surface, whereas at gold, the orientation has a tilt angle of approximately 30^{o} relative to the surface.[50, 51]

Bovine CCO is isolated according to the Soulimane and Buse Triton X-100 preparation.[52] Cytochrome c oxidase is then incorporated into a lipid bilayer membrane on a quartz crystal gold electrode using a procedure developed for reconstituting CCO into vesicles in solution involving cholate dialysis.[53] The Soulimane and Buse isolation procedure for CCO was selected because this preparation produces maximal turnover numbers, $k_{max} \geq 600\ s^{-1}$, which is similar to the maximum activity of CCO in the mitochondrial membrane.[52]

The phospholipids/isolated dimer contents in the Triton X-100 preparation are similar to the *in vivo* contents and contained phosphatidylethanolamine, phosphatidylcholine and cardiolipin as

the major constituents. This lipid content is relevant since it has been suggested by other research groups that CCO activity depends on the hydrocarbon environment of the membrane (usually favored by C18:1 unsaturated hydrocarbon tails) and that cardiolipin is essential for maximal CCO activity.[54-58] Tsukihara et al. found that the crystal structure of bovine heart CCO revealed 13 different polypeptide subunits with a calculated monomer molecular mass of 204,005 kD.[59, 60] Located within the subunits were two hemes, three coppers, one magnesium, and one zinc atom, and located at the surface were eight lipids (five phosphatidyl ethanolamines, three phosphatidyl glycerols) and two cholates. Cardiolipin was not detected in their x-ray crystallography method, but the intermonomer space was not examined and may contain room for several cardiolipins.[59] Using SDS/page, Soulimane and Buse demonstrated that their isolation technique revealed CCO to have 13 polypeptide subunits in agreement with the known literature.[59-63] Bovine CCO normally exists as a dimer, and microscopy techniques have suggested an asymmetrical distribution in the inner mitochondrial membrane. Depending on the microscopy technique used CCO protrudes as much as 60 – 80 Å on the cytosolic side and very little on the matrix surface side, about 10 – 20 Å.[64-67] Taniguchi determined that the gold crystal surface was not atomically smooth and had valleys 50 Å deep and peak to peak distances of 300 Å (results not published but acknowledged in reference 1). This gives enough room for the matrix side of immobilized CCO and provides room for a thin layer of trapped water molecules between the bilayer and the metal surface. Tapping mode scanning force microscopy (TM-SFM) images of the CCO modified electrodes are shown in PICTURE 1 below.[2]

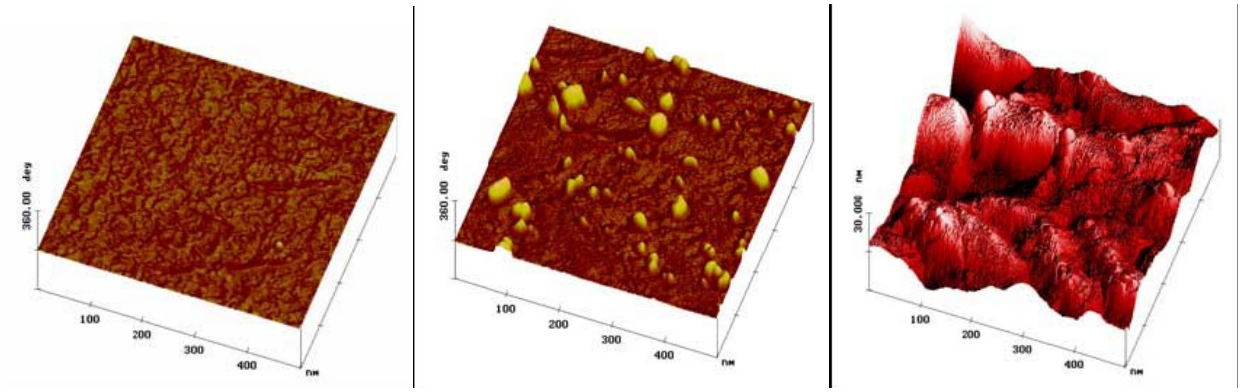

PICTURE 1: TM-SFM Images of modified electrodes were taken in air using a Digital Instrument Nanoscope IIIa, and were acquired at Iowa State University in Marc Porter's Group.[2] Left: Phase contrast image of LBM without CCO. Middle: Phase contrast image of LBM with CCO. Right: Topographical image of LBM with CCO. The measurement scale is 500 nm by 500 nm.

f. Additional analytical methods

To supplement the electrochemical data obtained from the CCO modified electrode two other confirmation methods were pursued. First was a new analytical method for the detection of free cyanide in water or phosphate buffer samples using metmyoglobin. A simple and quick method was desired for confirmation of cyanide concentrations before and after exposure to CCO. Myoglobin is a small heme protein (MW 17,800) found primarily in cardiac and skeletal muscle that is used to store dioxygen and to assist in the delivery of dioxygen to the mitochondria.[68-70] Myoglobin with its heme iron in the +3 state is known as metmyoglobin ($Mb(III)H_2O$) or

aquomyoglobin (since water is bound as the sixth ligand). Cyanide will displace the bound water molecule and bind to the heme iron forming cyanometmyoglobin ($Mb(III)CN^-$):[71]

$$Mb(III)H_2O + CN^- \leftrightarrow Mb(III)CN^- + H_2O$$

When dissolved in water or phosphate buffer myoglobin exists primarily as $Mb(III)H_2O$ without further preparation. If a sample blank can be obtained without cyanide, the solution should provide a baseline for matrix effects.

The second method pursued was the use of the fiber optic probe to measure UV or visible absorption changes in the oxidation of reduced cytochrome c, the natural redox partner for CCO. The current response from CCO is suppressed when bound to cyanide.[8] It will be exciting to monitor and to compare UV/visible absorption changes of the oxidation of reduced cytochrome c with the current response simultaneously when interacting with CCO and CCO bound with cyanide.

g. Henry's gas law constant for cyanide

Since cyanide has a pKa of 9.2, samples with a pH of lower than 9.2 will tend to lose cyanide as hydrogen cyanide to the atmosphere. Henry's Law describes the solubility of a gas in water under dilute conditions and low pressure, and the general form of Henry's Law is written as:

$$k_H = \frac{c_a}{p_g}$$

where c_a is the concentration of a species in the aqueous phase and p_g is the partial pressure of that species in the gas phase. Henry's law shows that the concentration of a solute gas in a solution is directly proportional to the partial pressure of that gas above the solution at equilibrium**.** Henry's law may also be expressed as a function of temperature and is described as:[72]

$$k_H = k_H^\theta \bullet \exp\left(\frac{-\Delta_{so\ln}H}{R}\left(\frac{1}{T} - \frac{1}{T^\theta}\right)\right)$$

where, $\Delta_{so\ln}H$ is the enthalpy of solution, T^θ is standard condition temperature (298.15 K)

and the temperature dependence is given by $\frac{-d\ln k_H}{d\left(\frac{1}{T}\right)} = \frac{\Delta_{so\ln}H}{R}$.

Cyanide Species	k_H^θ [units: M/atm]	$\frac{-d\ln k_H}{d\left(\frac{1}{T}\right)}$ [units: K]
CN^-	8.0×10^{-2}	1400
HCN	9.3 1.2×10^1 7.5	5000

The values listed are from different references cited in Dr. Sanders compilation of Henry's gas law constants.[72]

II. Materials and Methods:

a. Equipment

Spectrophotometric measurements were obtained using a Varian Cary 50 (Palo Alto, CA). An electrochemical quartz crystal microbalance (QCM), model CHI430A – (CH Instruments, Austin, TX), was used to measure quartz frequency changes and electrochemical measurements. Solution flow rates were controlled using a Harvard Apparatus (Holliston, MA) Model 11 syringe pumps, and solutions were prepared using ultra pure water that was purified using a Direct-Q3 system (Millipore Corporation, Billerica, MA) to exhibit a resistivity of 18.2 MΩ cm. The pH of the solutions was measured using a Corning model 440 pH meter (Woburn, MA). The Ag/AgCl, 1 M KCl reference electrodes were made in house and calibrated using a platinum wire immersed in a saturated solution of quinhydrone (Sigma-Aldrich, St. Louis, MO) of known pH.[73] Additional equipment obtained, which will be used in future work, is also listed in Appendix A.

b. Quartz Crystal Electrodes

Gold QCM electrodes (made to oscillate at 10 MHz) were purchased from International Crystal Manufactures Co. (Oklahoma City, OK) and consist of 1000 Å of vapor-deposited gold on polished quartz with a 50 Å chromium adhesion layer between the gold and quartz. The QCM electrodes geometric area is 0.2 cm^2. Prior to use, the gold QCM electrodes were first rinsed with absolute ethanol and then DI water, blown dry with research grade nitrogen and then placed in an ultraviolet light surface cleaner purchased from Novascan (Ames, IA). Ozone was generated for 5 minutes and then removed 55 minutes later by applying a vacuum through an ozone neutralizer attached to the ultraviolet light surface cleaner.

c. Silver Deposition

In earlier work approximately 1.6 monolayers of silver (1mM $AgNO_3$ 99.999%, Sigma-Aldrich, St. Louis, MO) was electrochemically deposited onto the electrode surface using an asymmetric double potential step method.[1] The Ag/AgCl, 1 M KCl reference electrode is isolated in a 1 mM $AgNO_3$ chamber to prevent AgCl deposits on the working electrode surface. An initial potential of +500 mV is applied to obtain a stable baseline and then stepped to +300 mV to initiate silver deposition. Both the current and frequency shift are monitored during deposition. The potential is

stepped to approximately +400 mV to stop silver deposition. The in-house built potentiostat used in the earlier work allowed potential control during the experiment. However, with CH Instrument's potentiostat, the user cannot control the potential during the experiment and one is limited to initial parameter settings. Therefore several experiments would have to be performed to duplicate the asymmetric double potential step. Due to an error in the initial parameter settings, which were copied from experiment to experiment, the results described within refer to several monolayers of silver deposited on the gold surface instead of 1.6 monolayers. After depositing silver the electrode is first tripled rinsed with Direct-Q purified water, then rinsed with ethanol and then dried with research grade nitrogen in preparation for the octadecyl mercaptan deposition. Cyclic voltammograms from -100 mV to +300 mV may be obtained in phosphate buffer (0.1 M, pH 7.4) to characterize the deposited silver layer and to compare the double layer capacitance.

d. Octadecyl Mercaptan Deposition

Absolute ethanol (4 ml) is added to the cell, and research grade nitrogen is allowed to gently bubble in the ethanol through a stainless steel needle (22 gauge, blunt tip) placed about 2 mm below the surface. The electrodes are then allowed to equilibrate with the ethanol until a stable baseline frequency is observed. Once a stable baseline is achieved 50 µl of 500 µM OM will be added to the ethanol (giving an OM concentration of 6.25 µM) just below the nitrogen agitation. Approximately 24 ng of OM will be deposited onto the electrode surface with the aid of the QCM to monitor frequency changes of approximately 21 Hz giving approximately 0.5 monolayer coverage. This QCM frequency shift is used to know when to remove the QCM electrodes from the reacting solution to control the OM coverage. The reaction is quenched by rinsing the cell with absolute ethanol and Direct-Q purified water. The average reaction time of 21 experiments, for a 0.5 monolayer of OM, was determined to be 10.64 ± 4.42 minutes by Burgess with the variations attributed to the gentle nitrogen bubbling.[1]

e. Sauerbrey Equation

The correlation of frequency change and mass change as described by the Sauerbrey equation was investigated by Burgess et al.[1]

Sauerbrey Equation $$\Delta F = \frac{-2f_o^2 \Delta m}{A(\upsilon_q \rho_q)^{1/2}}$$

where $2f_o^2 / A(\upsilon_q \rho_q)^{1/2}$ corresponds to the QCM sensitivity constant. Burgess et al. determined that the QCM sensitivity constant calculated from silver deposition charge/frequency shift data (1.11 Hz/ng) is in good agreement with that predicted by the Sauerbrey equation[74, 75] (1.13 Hz/ng) and that the sensitivity constant was also independent of the silver deposition potential. Based on the QCM sensitivity constant calculated from the silver deposition experiments, a 21 Hz shift in QCM frequency corresponds to formation of half of a monolayer of OM.

f. Preparing Lipid Solution

The lipids DOPE (1,2-Dioleoyl-sn-glycero-3-phosphoethanolamine - MW 744.04 (500 mg) 18:1PE) and DOPC (1,2-Dioleoyl-sn-glycero-3-phosphocholine - MW 786.15 (500 mg) 18:1PC) are obtained from Avanti Polar Lipids**, (**Alabaster, AL) in chloroform storage solvent. The lipid solution is prepared using 2.5 ml DOPE and 0.3 ml DOPC in a round bottom flask wrapped in aluminum foil to avoid photodegradation. The chloroform is removed from the DOPE and DOPC mixture using a stream of filtered research grade nitrogen. Then 50 mg of sodium deoxycholate (Sigma-Aldrich, St. Louis, MO) is added to the round-bottom flask with 3 ml of 0.1 M phosphate buffer, pH 7.4 and allowed to stir at 4 °C with agitation until the lipids are solubilized. The lipids are then treated with Chelex-100 (ion-exchange resin, BioRad, Hercules, CA) for ca. 12 hours at 4 °C with agitation to remove metal cation contaminants. The Chelex-100 is then removed by filtration (UNIFLO plus 0.2 *í*mCA and glass fiber) from the deoxycholate-lipid solution. The final stock lipid solution is composed of 11 mM DOPE, 2 mM DOPC and 40 mM sodium deoxycholate and stored at -80 °C.

g. Preparing the CCO Modified QCM electrodes

Bovine CCO that was isolated using the Soulimane and Buse procedure[52] by Dr. Bertha C. King, Dr. Zoia Nikolaeva, and Professor Mikhail Smirnov was obtained from Dr. Fred Hawkridge's group at Virginia Commonwealth University.

Bovine CCO is incorporated into a lipid bilayer membrane on the electrode surface by mixing equal volumes of a 2 mg/ml solution of CCO (solubilized in 1 mM Tris/HCl, pH 7.6, 0.1% Triton X-100) and a lipid solution composed of 11 mM DOPE, 2 mM DOPC and 40 mM sodium deoxycholate. The anionic detergent sodium deoxycholate is used in the dialysis procedure to solubilize the protein lipid mixture. The mixture is then injected into the sample chamber of a dual-chambered electrochemical dialysis cell to prepare the CCO lipid bilayer membrane on the electrode surface. The molecular porous membrane tubing with molecular weight cut off (MWCO) 3500 (Spectrum Laboratories, Rancho Dominguez, CA) was used as a dialysis membrane and is soaked in water to remove glycerin and sulfides from the membrane prior to use. Phosphate buffer (0.1 M, pH 7.4, ACS reagent grade) is then allowed to flow through the dialysis chamber of the cell for 18 hours at a flow rate of 25 μl/min. Then phosphate buffer (0.1 M, pH 7.4) is introduced to the sample chamber for approximately 20 hours at a flow rate of 5 μl/min to remove any excess sodium deoxycholate. Observation of a typical immobilized CCO voltammogram (i.e., large oxidative current as compared with lipid bilayer only electrode) indicates CCO activity and the endpoint of CCO and bilayer formation.[1-8]

Cytochrome c (Sigma-Aldrich, St. Louis, MO) is reduced with sodium dithionite and desalted using a 5 ml high-trap size exclusion column (Amersham, Piscataway, NJ). The concentration of reduced horse heart cytochrome c can be determined spectrophotometrically using a molar absorptivity (λ_{max} = 550 nm) of 29,500 $M^{-1}cm^{-1}$.[76, 77]

h. Preparing stock metmyoglobin solutions

Horse heart myoglobin (Sigma-Aldrich, St. Louis, MO) was prepared by dissolving approximately 0.05 grams of myoglobin in 10 ml of 0.1 M phosphate buffer, pH 7.4 at room temperature. The sample was then filtered using Whatman No. 41 filter paper and stored at 4 °C when not in use. Further preparation of myoglobin was not necessary since all of the dissolved myoglobin is metmyoglobin. All dilutions from the stock $Mb(III)H_2O$ were performed using 0.1 M phosphate buffer, pH 7.4. The $Mb(III)H_2O$ concentration was determined using Beer's Law, $A = \varepsilon bc$, where ε is the molar absorptivity ($M^{-1}cm^{-1}$), b is the pathlength (cm) and c is the molar concentration (M). The molar absorptivity for $Mb(III)H_2O$ is 188,000 M^{-1} cm^{-1} at 409 nm.[78] The cyanide solutions were prepared from sodium cyanide (Sigma-Aldrich, St. Louis, MO) in a basic solution of sodium hydroxide (Sigma-Aldrich, St. Louis, MO) to minimize loss of cyanide. See Results and Discussion for sodium hydroxide concentrations used. Difference spectroscopy was applied since the absorbance spectrum for $Mb(III)H_2O$ and $Mb(III)CN^-$ overlap. The absorbance values at 409 nm are subtracted and applied to Beer's law in the difference form, $dA = (d\varepsilon)(db)(dc)$. Also see Results and Discussion for determination of the molar absorptivity value for $Mb(III)CN^-$.

III. Results & Discussion:

The results obtained thus far deal with equipment setup and operation, preparing the CCO bilayer electrode and a new method for cyanide measurement in solution using metmyoglobin.

a. QCM Reference Oscillator

As described in the Method and Materials section the QCM is used in the preparation of the electrode surface before incorporation of CCO in a lipid bilayer on the electrode surface. Previous work by Hawkridge and coworkers[1-8] used a QCM housed in a Faraday cage, built in house based on the circuitry design published by Bruckenstein et al.[74, 79] and controlled using Lab View™ software (National Instruments, Austin, TX). A commercially equivalent QCM purchased from CH Instruments did not work initially. The operational failure of the QCM was found to be due to the 8 MHz reference oscillator in the electronics of the QCM and the use of 10 MHz electrode crystals. Several companies indicated that a 10.005 MHz oscillator crystal with the exact same output logic would require custom manufacturing, take several months to produce and would require bulk pricing. Therefore the programmable JITO-2 reference oscillator (Mouser electronics, Mansfield, TX) with a reference frequency of 10.005 MHz was considered since bulk shipment or custom pricing was not required and delivery time was estimated to be less than two weeks. CH Instruments was unable to specify whether the JITO-2 would work with their electronics due to the different output logics. The JITO-2 was ordered and appears to work well with the QCM electronic circuit. The company was notified so that future customers may be informed when facing the same situation. The reference oscillator's specifications are shown in Appendix B.

b. Octadecyl Mercaptan Deposition

As explained in the introduction the deposition of OM is necessary to give a hydrophobic region above the electrode surface for interaction with the hydrophobic region of the lipid bilayer and enzyme, which results in a more stable bilayer. Initially, characterization of the silver surface using cyclic voltammetry in 0.1 M, pH 7.4, phosphate buffer, was used to determine the extent of contamination of the electrode surface after silver deposition and as a reference for double layer capacitance changes for the OM deposition. For example the presence of current peaks in the potential window would likely indicate that silver chloride was formed during the silver deposition step. However, this surface characterization may have caused the electrode surface to be coated with phosphate anions, including PO_4^{3-}, even though its concentration is extremely small (less than 10^{-12}). When the surface is characterized with phosphate buffer the frequency change does not necessarily increase with deposition time and was found to take 10 minutes or so longer, which is in the timeframe published in earlier work[1] (FIGURE 1). However, if the silver characterization step is left out, the OM deposition (~ 21 Hz shift) occurs much faster and in less than two minutes (FIGURE 2). In addition the frequency change was found to be linear with deposition time in this case (FIGURE 3). Reproducibility will depend on other variables, and the flux of the OM to the surface will be affected by placement of the stainless steel needle, nitrogen agitation, ethanol equilibration time, temperature changes, and OM concentration. Precise control of these other variables will help enable the comparison of electrode surface effects.

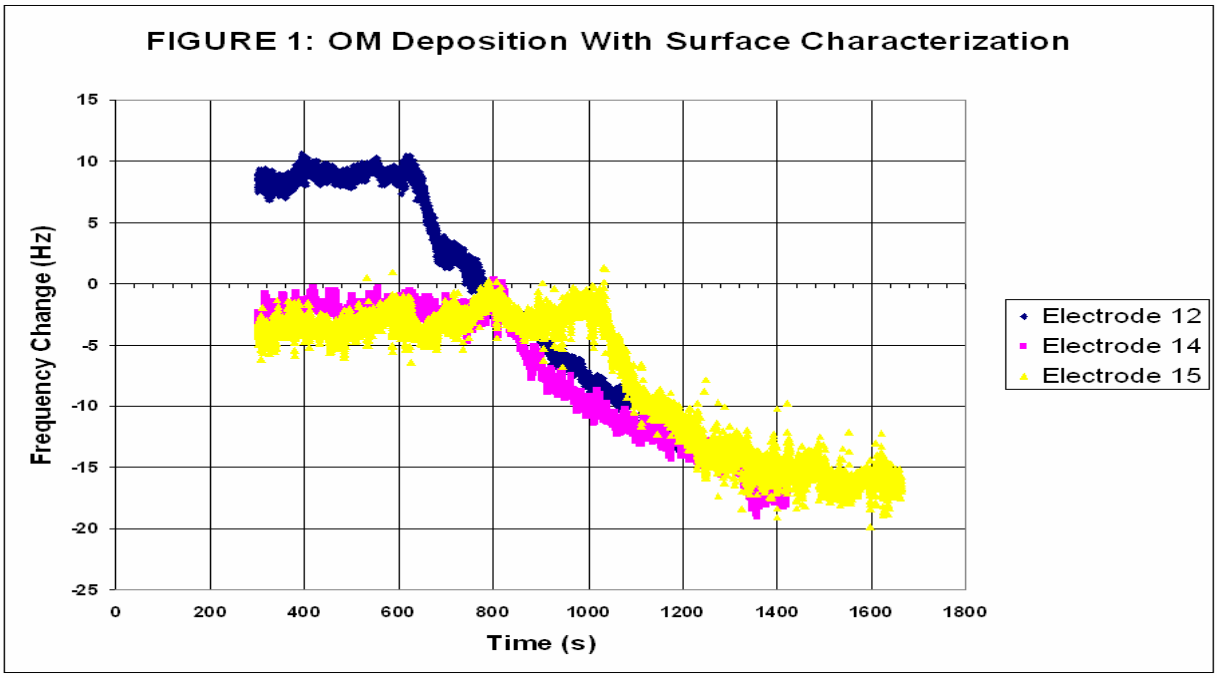

	OM Injected at Time	Total Deposit Time	Approx. Freq. Change
Electrode 12	600 s	600 s	20 Hz
Electrode 14	800 s	621 s	16 Hz
Electrode 15	1000 s	664 s	16 Hz

FIGURE 1. OM deposition with characterization of the electrode surface with cyclic voltammetry in 0.1 M Phosphate buffer, pH 7.4 after the silver deposition step.

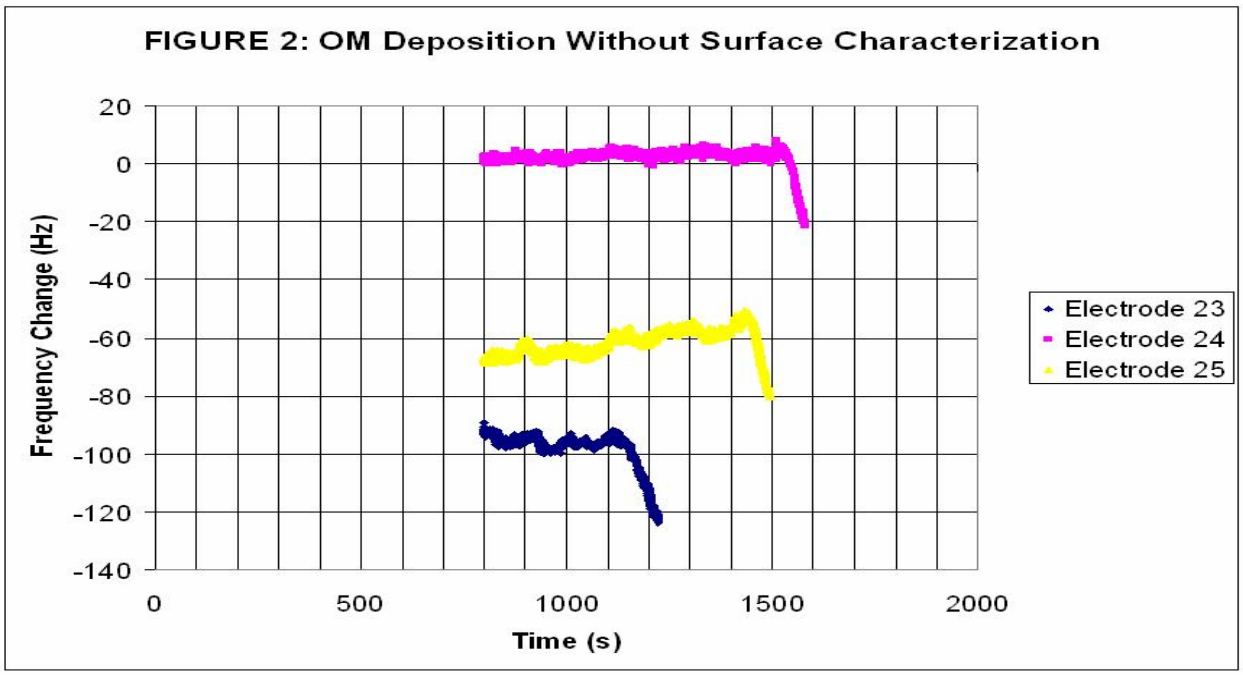

	OM Injected at Time	Total Deposit Time	Approx. Freq. Change
Electrode 23	1100 s	125 s	30 Hz
Electrode 24	1500 s	81 s	24 Hz
Electrode 25	1400 s	93 s	26 Hz

FIGURE 2. OM deposition without characterization of the electrode surface with cyclic voltammetry in 0.1 M phosphate buffer, pH 7.4 after the silver deposition step.

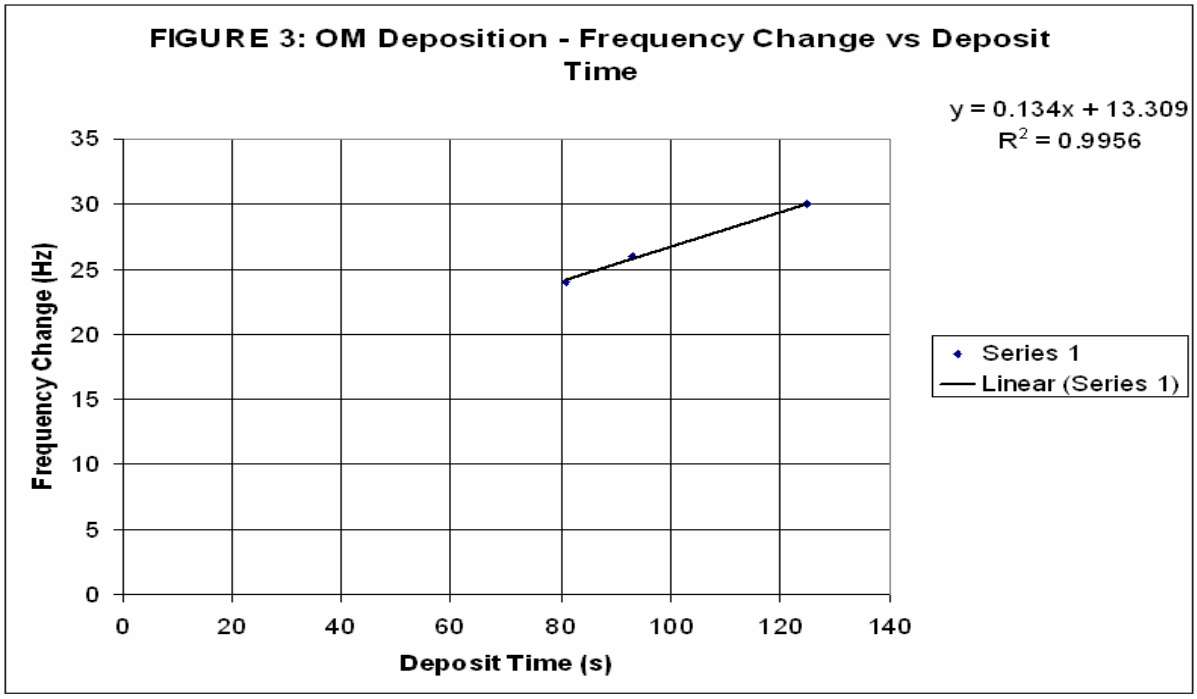

FIGURE 3. The Frequency change versus Deposit time from FIGURE 2.

c. Interference in cyclic voltammetry of CCO

A source of contamination appeared in the cyclic voltammetry scans of the CCO electrode (FIGURE 4a & 4b). The peak shapes shifted in location and size, a second reduction peak occasionally appeared and the peaks were sometimes sharp even though the cyclic voltammetry parameters remained constant. Attempts were made to determine the source of contamination. For example, the dialysis cells, flow lines and fittings were cleaned thoroughly with detergent and ethanol and then rinsed with DI water; flow lines and fittings were replaced and a new dialysis cell was used; and glassware containing stock solutions were cleaned and all solutions were freshly prepared.

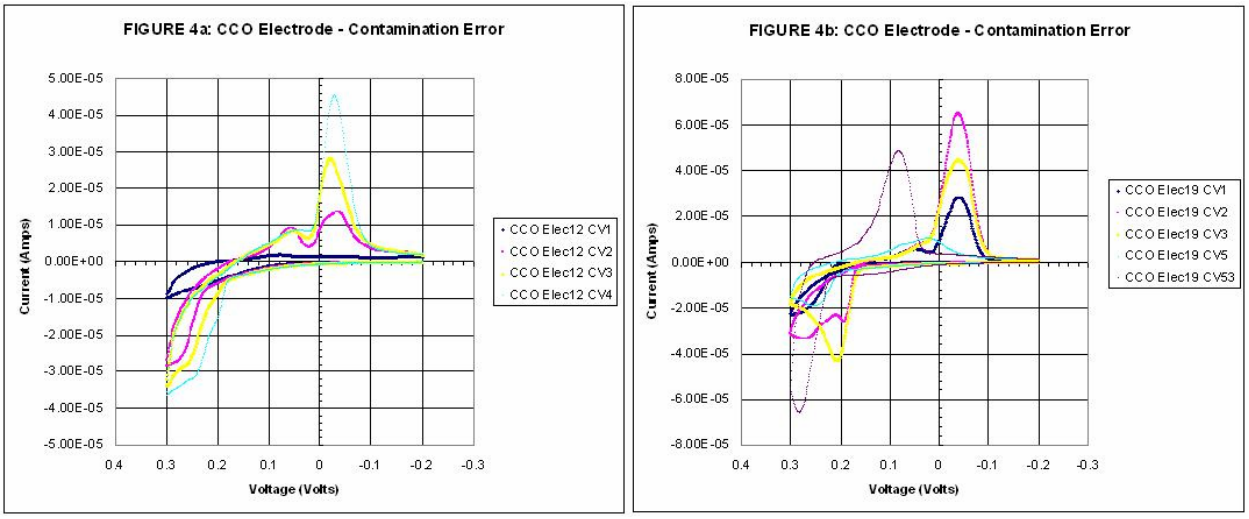

FIGURE 4a & 4b. Different electrodes illustrating a source of contamination in the cyclic voltammetry scans of the CCO electrode. The peak shapes shifted in location and size, a second reduction peak occasionally appeared and the peaks were sometimes sharp even though the cyclic voltammetry parameters remained constant.

After the initial attempts to eliminate the source of contamination in CCO cyclic voltammograms failed, a blank lipid electrode was prepared to see if peaks would be present. The peaks found indicated that either the lipids were highly contaminated or chloride from the reference electrode was reacting with the silver monolayer to form silver chloride (FIGURE 5a). Since Chelex-100 resin was used to remove possible contaminants from the lipids and the lipids had been remade several times according to earlier published work[3] the reference electrode was examined as the source of interference. To do this a double junction electrode was used to examine the same electrode used in FIGURE 5a where the outer reference contained 0.1 M, pH 7.4 phosphate buffer and the inner reference electrode contained 1 M KCl. The resulting cyclic voltammogram when a double junction electrode was used is illustrated in FIGURE 5b. The peaks were eliminated, suggesting that chloride from the single junction reference electrode was reacting with silver in the potential window of the experiment. To double check this result the double junction reference electrode was removed and a single reference electrode was again used. The interfering silver chloride peaks again appeared in the cyclic voltammogram, confirming this hypothesis. (FIGURE 5c). Surface characterization of the electrode surface before the addition of lipid or lipid and enzyme is illustrated in FIGURE 5d. Cyclic voltammograms of the bare gold surface, the silver deposition and OM deposition suggest a clean surface for every electrode and deposition step that was characterized. The decrease in double layer capacitance is as expected for the ½ monolayer of OM. A cyclic voltammogram from FIGURE 5b, CV6, a lipid only electrode, was compared to these surface characterizations in FIGURE 5e. The capacitance of the lipid only electrode was approximately the same for the OM deposition, which suggests a poor blocking film or that the bilayer did not form on the surface at all. FIGURE 5f is a combination of cyclic voltammograms from FIGURES 5a – 5e for current scale comparison.

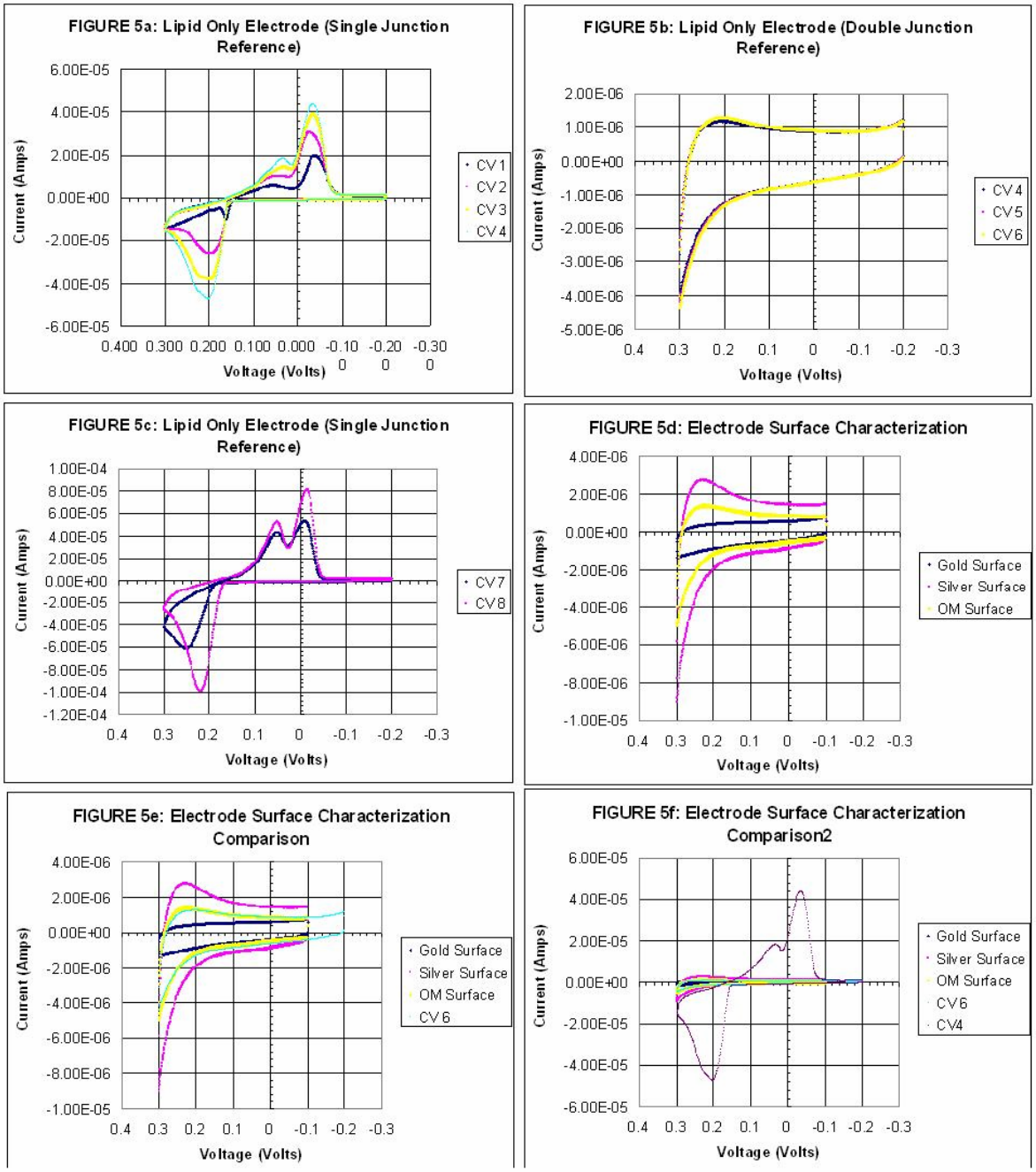

FIGURE 5(a-f). Determining interference peaks in cyclic voltammograms of the lipid only electrode.

A new lipid-only electrode was then prepared in which the reference electrode did not contain 1M KCl and contained phosphate buffer during the bilayer formation. After the bilayer formation a double junction reference electrode as described earlier was also used in the cyclic voltammetry measurements. No silver chloride interference peaks were found (FIGURE 6a). In addition a comparison of the double layer capacitance of the lipid bilayer and the double layer capacitance of the initial electrode surface characterizations showed a decrease, indicating a

much better blocking film by the bilayer (FIGURE 6b). Note, the gold surface characterization CV displayed in FIGURES 5d, e and 6b were performed in 0.1M KNO_3.

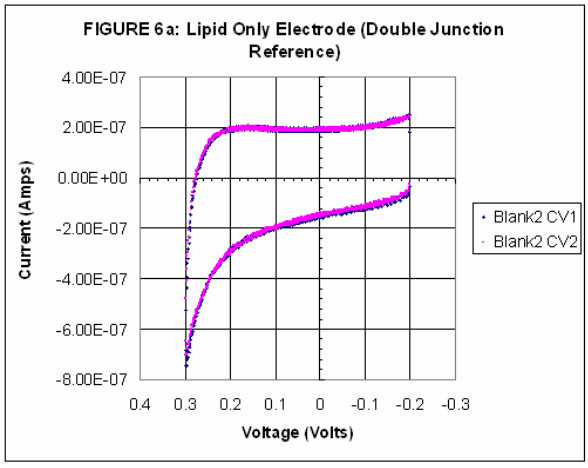

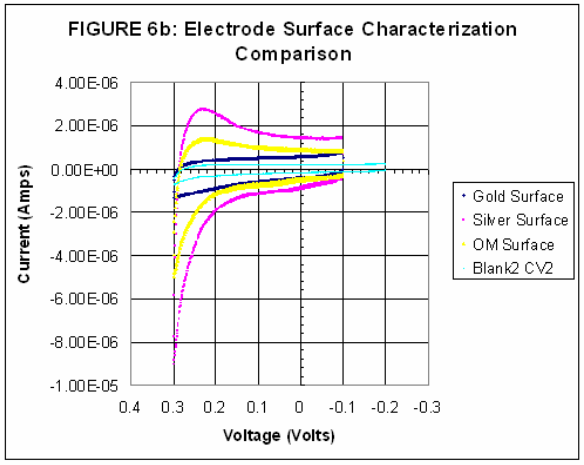

FIGURE 6. Lipid only electrode characterization using a double junction reference electrode and filling the single reference electrode with 0.1 M PB, pH 7.4 phosphate buffer during bilayer formation.

The same procedure described in removing possible silver chloride interference was applied to incorporation of CCO in the bilayer. The resulting cyclic voltammograms are much more stable and obtain an identical current response within 3 cyclic voltammograms (FIGURE 7a). A comparison of the lipid only electrode and CCO electrode is illustrated in FIGURE 7b.

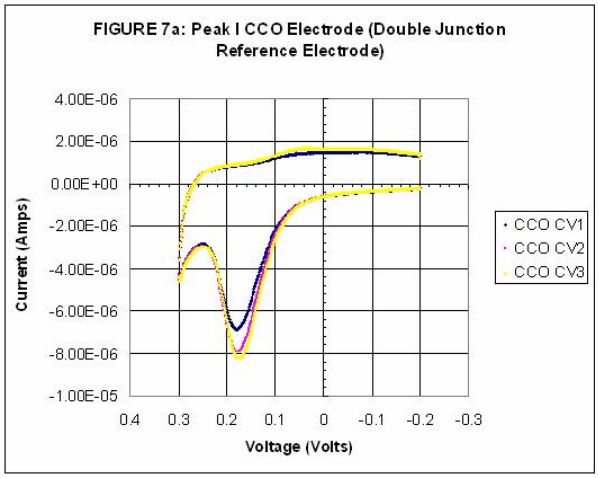

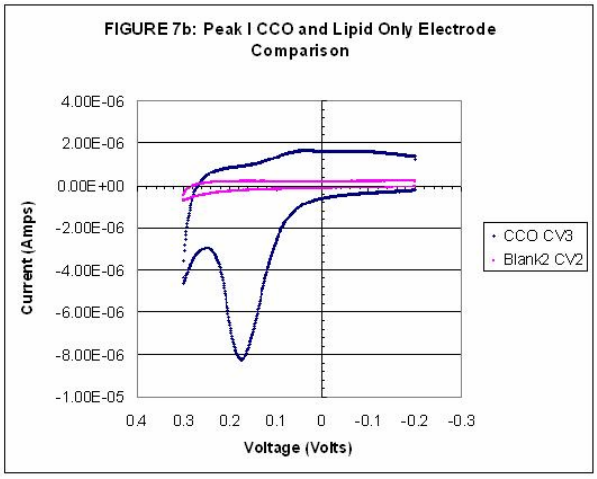

FIGURE 7. Cyclic voltammograms of CCO are much more stable when a double junction reference electrode is used and 1 M KCl is left out of the reference electrode during the enzyme / bilayer formation.

d. Spectroelectrochemistry Experimental Design

The dialysis cell was modified to hold a fiber optic probe that may be used to measure UV/visible changes of reduced cytochrome c (CCO's native redox partner) during its oxidation by CCO. After several rearrangements an experimental setup has been established. The experimental setup is housed in a Yamato (South San Francisco, CA) DKN400 convectional oven, which is used to maintain constant temperatures and to help eliminate cyclic frequency noise in QCM measurements. The fiber optic probe is held in place by loctite epoxy in a threaded ¼ in ID Swagelok stainless steel fitting. In addition, it is advisable to put a thin layer coat of epoxy on the stainless steel probe casing to ensure the metal does not come in contact with the auxiliary electrode. Before the setup is applied to the oxidation of reduced cytochrome c by CCO the limitations and parameters for optimizing spectroscopic and electrochemical measurements should be obtained using a simpler redox couple and environment. This is currently underway using the well-known ferri/ferro cyanide redox couple at a plain gold electrode.

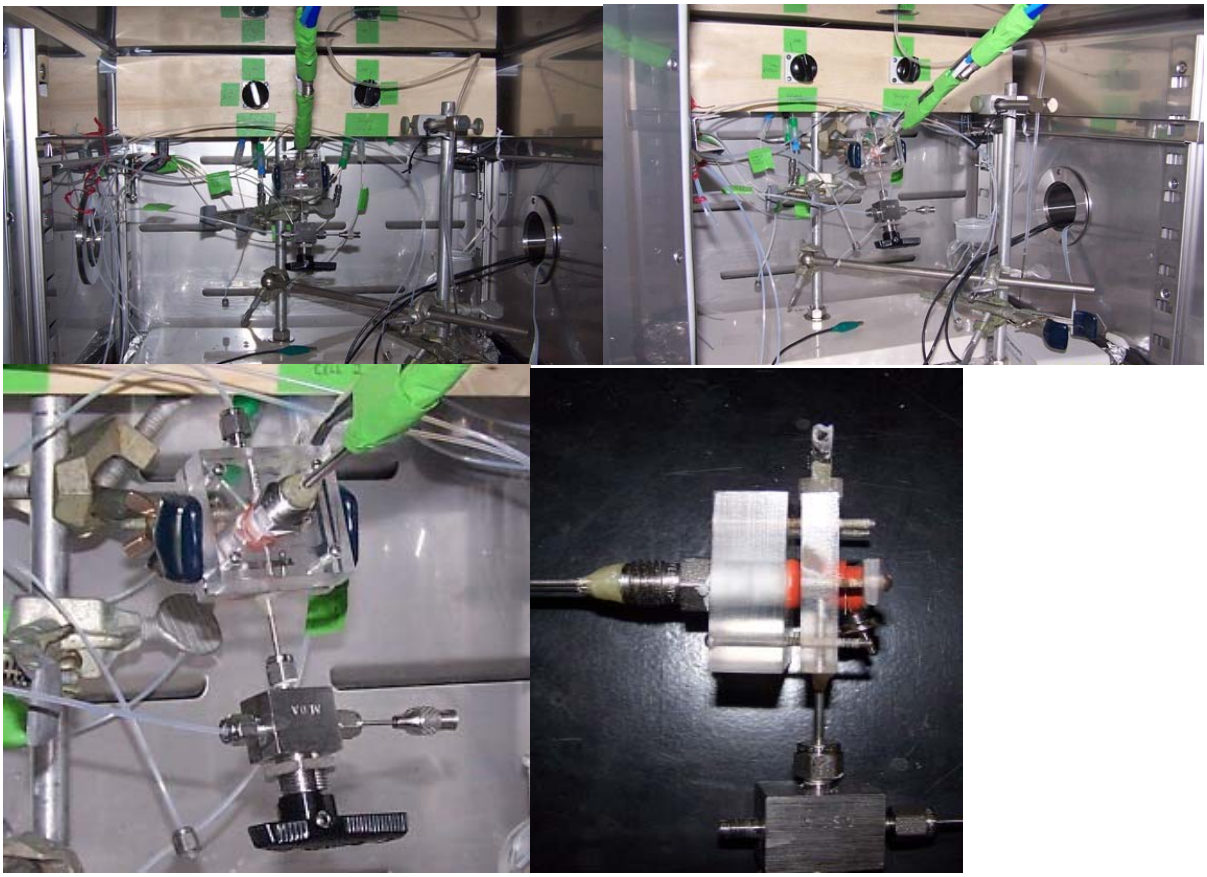

PICTURE 2. Spectroelectrochemistry Experimental Design.

e. Detection of Cyanide using metmyoglobin

The loss of cyanide can be minimized by preserving aqueous samples with sodium hydroxide to a pH of greater than 9.3. Therefore possible effects of different sodium hydroxide (NaOH) concentrations (sample pH) on Mb(III)H_2O dissolved in 0.1 M phosphate buffer, pH 7.4 were initially examined. In the following experiment a 200 µL of stock Mb(III)H_2O was added to 0.5 mL of each sample to examine pH effects on Mb(III)H_2O.

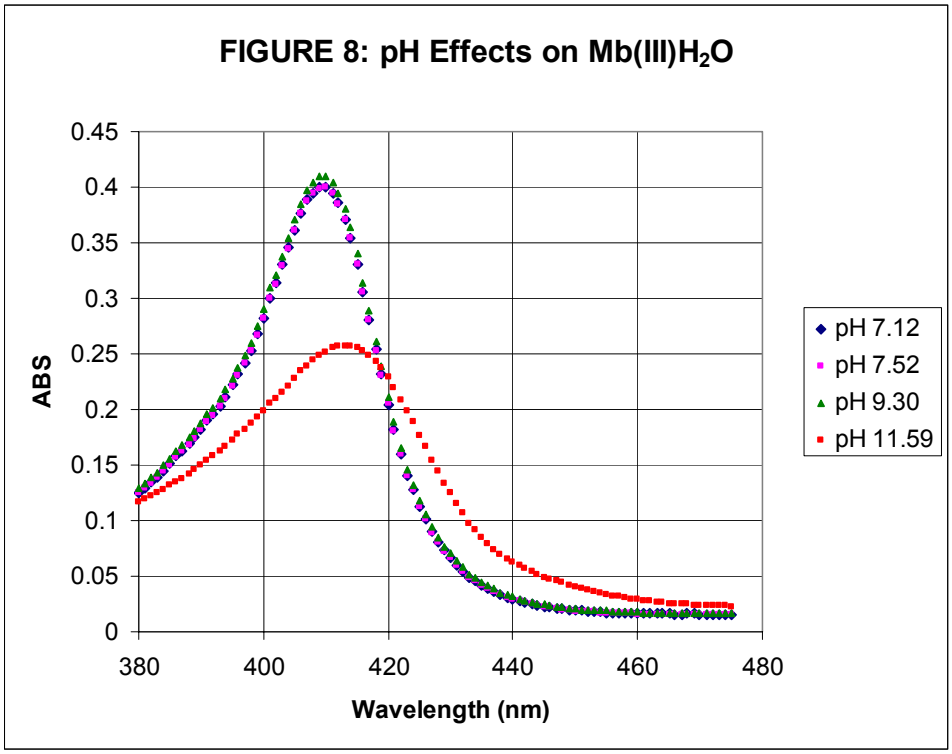

Sample	Amount of Well H_2O (mL)	NaOH Vol. Added (mL)	NaOH Conc. (Molar)	Final Sample Measured pH
1	10	0	NA	7.12
2	9	1	0.001	7.52
3	9	1	0.01	9.30
4	9	1	0.1	11.59

FIGURE 8. The effects on Mb(III)H_2O by samples preserved with different concentrations of NaOH.

The final solution pH of 11.59 caused a significant decrease in absorbance, which suggests that cyanide standards should not be made in 0.1 M NaOH and the pH of the sample should be lower. For the remaining experiments cyanide standard samples were prepared in either 0.01 M NaOH (pH =12) or 0.001 M NaOH (pH = 11) to minimize release of cyanide to the atmosphere before testing and to minimize denaturing effects of Mb(III)H_2O at higher sample pH.

In the next experiment 10 µl increments of 5 ppm CN^- in 0.01 M NaOH were added into a 1 cm cuvette containing 2.5 ml of Mb(III)H_2O dissolved in 0.1 M, pH 7.4 phosphate buffer. (A total volume of 350 µl CN^- was added.) Approximately 3 minutes after each addition of 10 µl of 5

ppm CN^- the ABS was measured and plotted in FIGURE 9. The ABS plot illustrates the isosbestic point demonstrating that the absorbing forms of $Mb(III)H_2O$ and $Mb(III)CN^-$ are interconvertible.

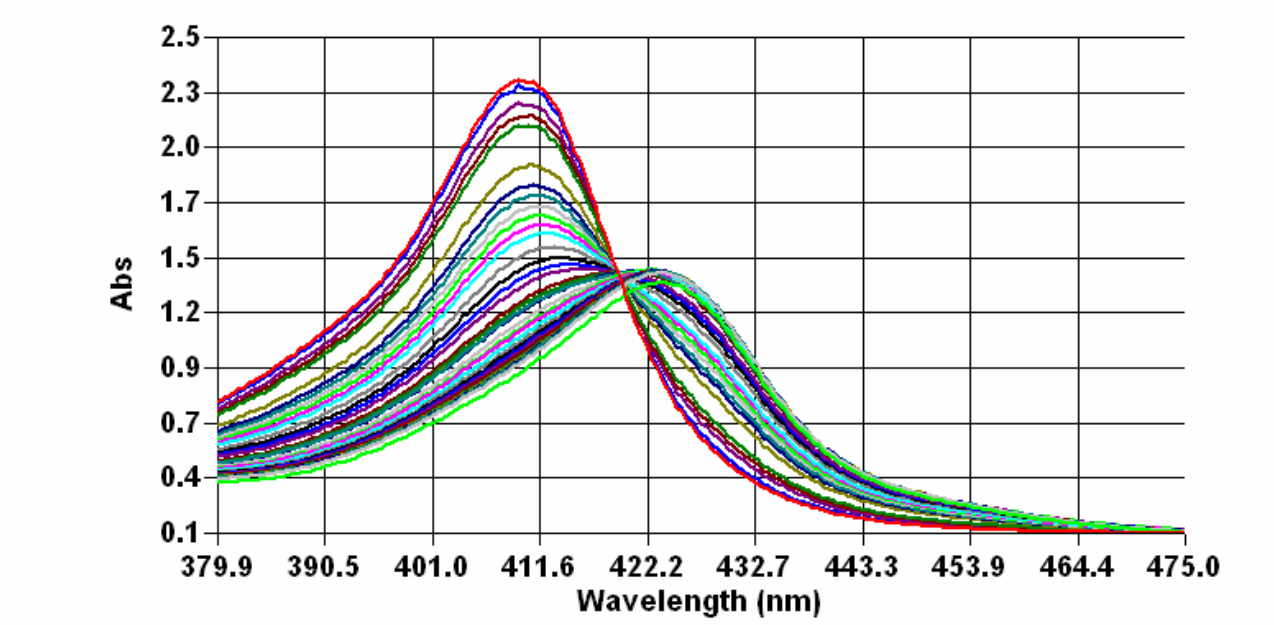

FIGURE 9. Titration of 5 ppm CN^- in 0.01 M NaOH with 2.5 ml of $Mb(III)H_2O$ dissolved in 0.1 M, pH 7.4 phosphate buffer.

The molar absorptivity for $Mb(III)CN^-$ was determined at 409 nm in two separate experiments. In the first experiment a volume of 0.5 ml of 1 M NaCN in 0.01 M NaOH was added to 2.5 ml $Mb(III)H_2O$ dissolved in 0.1 M, pH 7.4, phosphate buffer to ensure complete conversion to $Mb(III)CN^-$. Using a molar absorptivity of 188,000 M^{-1} cm^{-1} at 409 nm for $Mb(III)H_2O$ [78] and a pathlength of 0.1 cm the concentration of $Mb(III)H_2O$ was determined to be 12.2 x 10^{-6} M. After dilution the new $Mb(III)H_2O$ concentration was 10.2 x 10^{-6} M, which was used to calculate the molar absorptivity of ~ 82500 M^{-1} cm^{-1} at 409 nm for $Mb(III)CN^-$. The absorbance spectrum is plotted in FIGURE 10a. In the second experiment 200 uL of $Mb(III)H_2O$ stock solution (in 0.1 M, pH 7.4 phosphate buffer) was added to 500 µL of sample, which had the following constituents:

Samples	Well H_2O Volume (mL)	Cyanide Concentration (ppm)	Volume of 0.01 M NaOH added (mL)	Measured ABS at 409 nm
Sample 1	9	0	1	0.3998
Sample 2	9	650	1	0.1748

Again using a molar absorptivity of 188,000 M^{-1} cm^{-1} at 409 nm the concentration of $Mb(III)H_2O$ in sample 1 (without cyanide) was determined to be 21.2 x 10^{-6} M. Using this concentration a molar absorptivity of 82500 M^{-1} cm^{-1} at 409 nm for $Mb(III)CN^-$ was also calculated. ABS spectrum is plotted in FIGURE 10b.

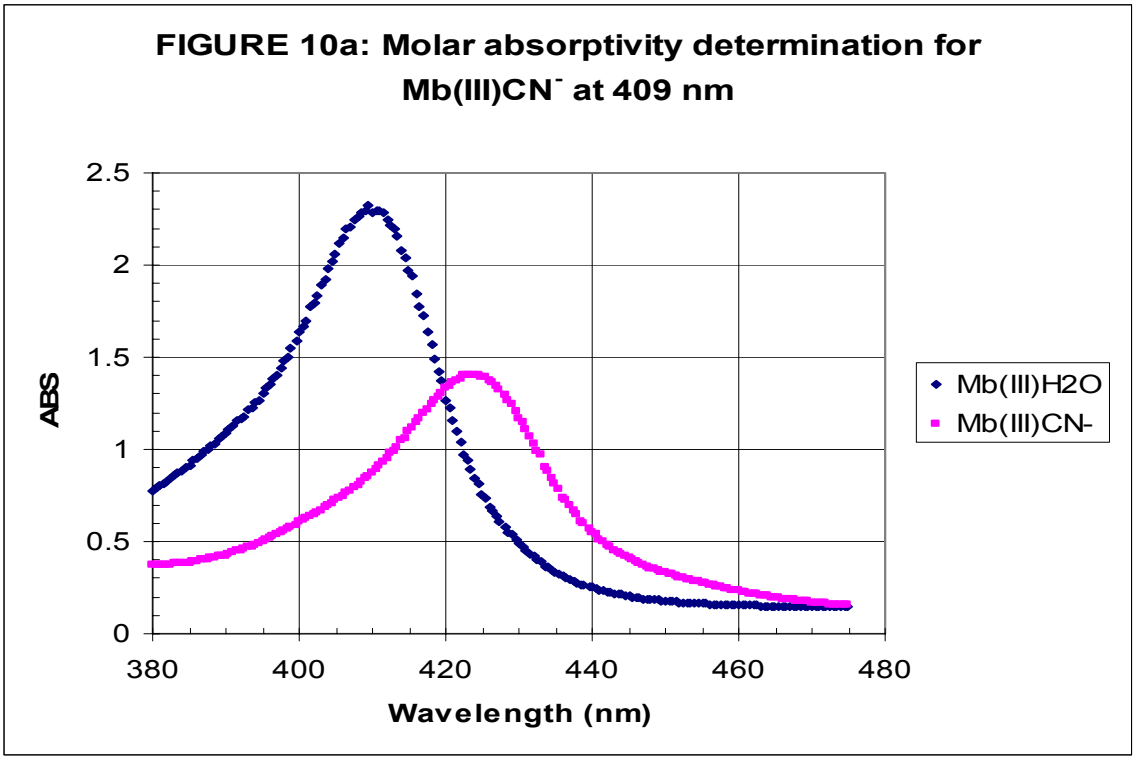

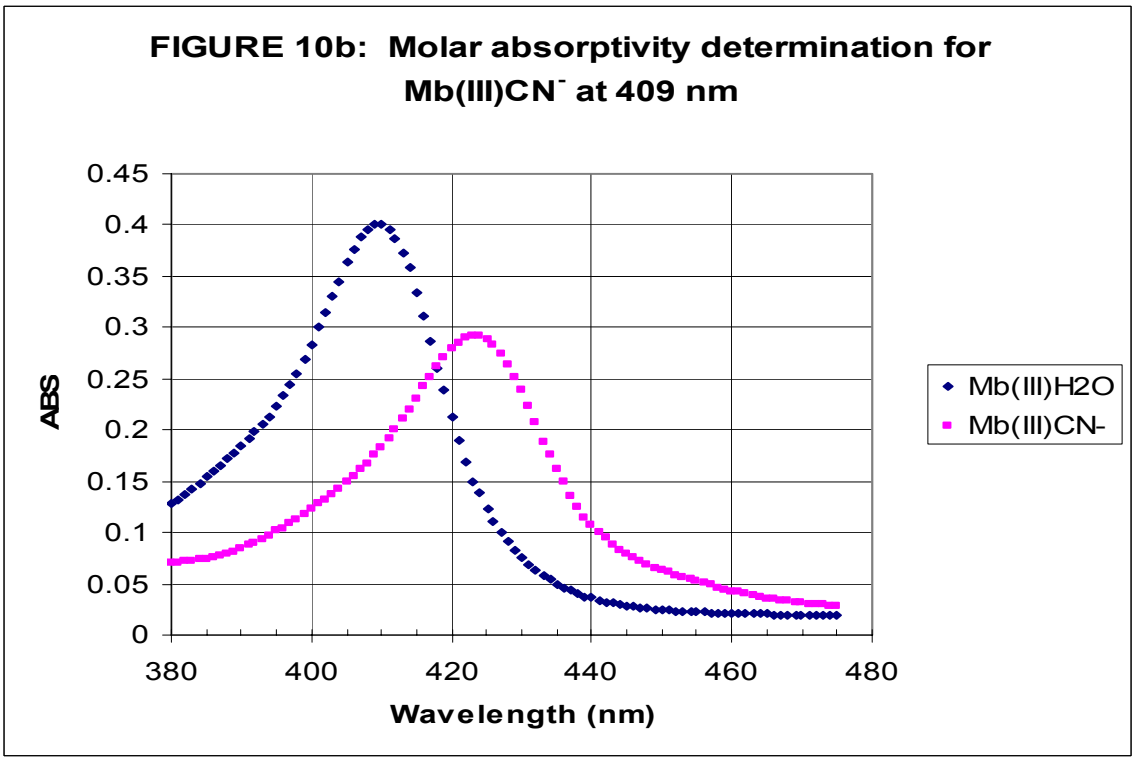

FIGURE 10a & 10b. Absorbance plots from experiments to determine the molar absorptivity of $Mb(III)CN^-$ at 409 nm.

In the following experiments a series of cyanide standards were made and measured using Mb(III)H_2O. The change in concentration plotted versus the cyanide standards measured resulted in a linear calibration curve. In the first experiment a series of standards were made in well water from a 10 ppm stock cyanide solution dissolved in 0.001 M NaOH. The pH of the blank sample was measured to be 7.66 using an Orion pH electrode. In a 2 mL Teflon vial 0.5 mL of the sample and 200 µL of stock Mb(III)H_2O was added. A portion of sample was added to a 0.1 cm cuvvette and the ABS was measured. Results are in FIGURE 11a. Since the spectra for the two species overlap the absorbance values at 409 nm are subtracted and applied to Beer's law in the difference form, $dA = (d\varepsilon)(db)(dc)$.

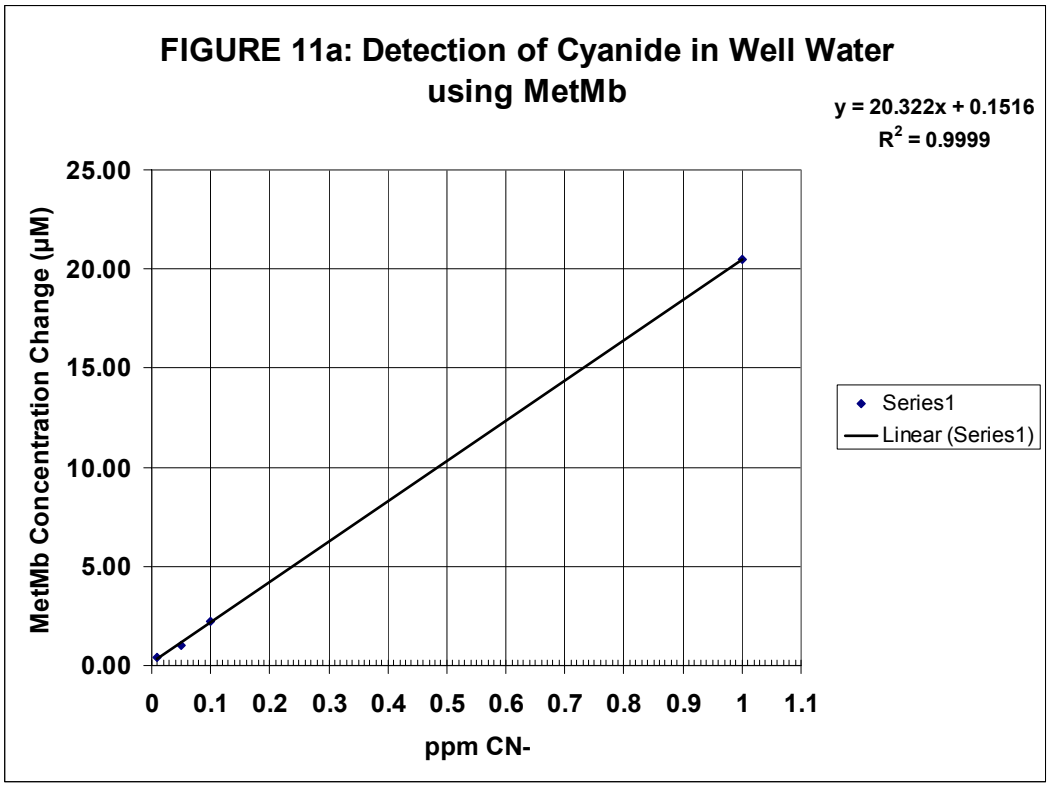

Samples	Well Water Volume (mL)	Volume of 0.001 M NaOH added (µL)	Volume of 10 ppm CN (in 0.001 M NaOH) added (µL)
Blank	9	1000	0
0.01 ppm CN	9	990	10
0.05 ppm CN	9	950	50
0.1 ppm CN	9	900	100
1 ppm CN	9	0	1000

Samples	Measured ABS at 409nm	dA	d ε	b	dC
Blank	0.4605				
0.01 ppm CN	0.4559	0.0046	105500	0.1	4.36E-07
0.05 ppm CN	0.4497	0.0108	105500	0.1	1.02E-06
0.1 ppm CN	0.4368	0.0237	105500	0.1	2.25E-06
1 ppm CN	0.2445	0.216	105500	0.1	2.05E-05

A second experiment was conducted in which a series of standards were made in well water from a 5 ppm stock cyanide solution dissolved in 0.01 M NaOH. The pH of the blank sample was measured to be 9.39 using an Orion pH electrode. In a 2 mL Teflon vial 0.5 mL of the sample and 200 µL of stock Mb(III)H_2O were added. A portion of sample was added to a 0.1 cm cuvette and the ABS was measured. Results are in FIGURE 11b.

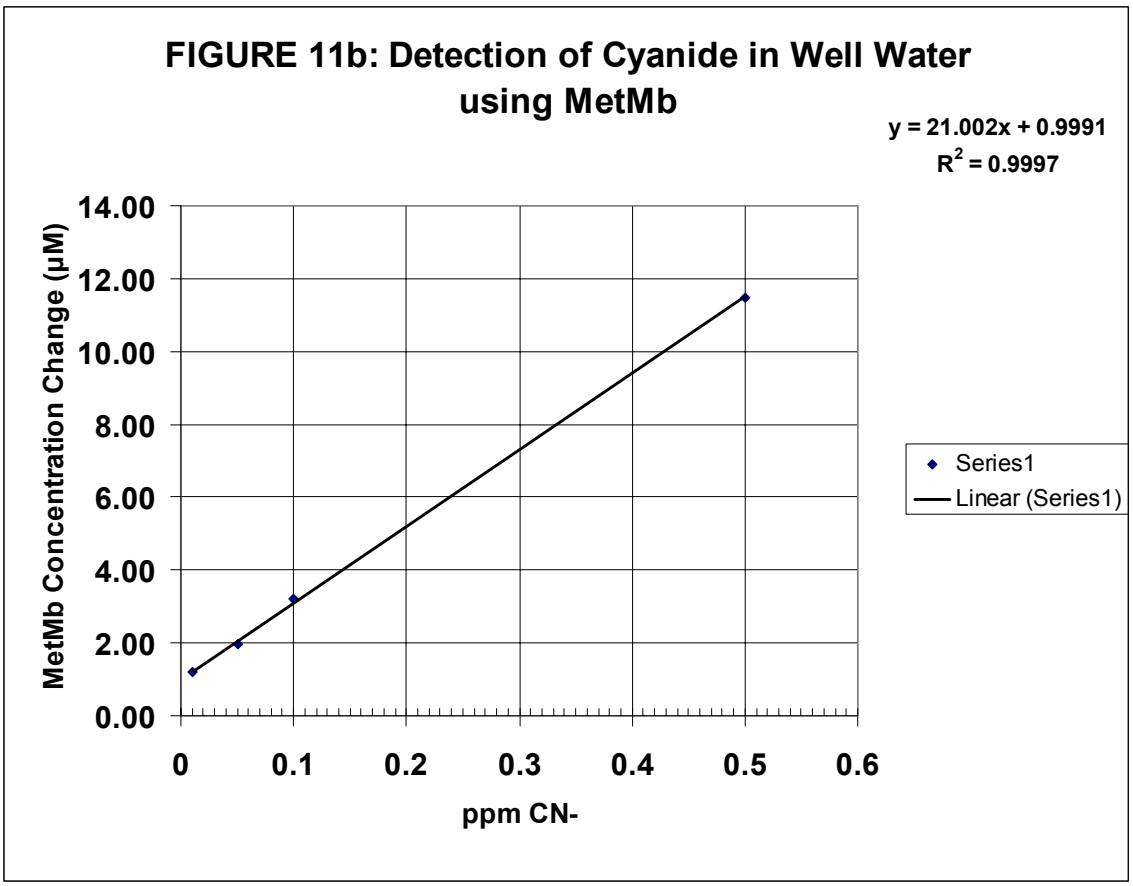

Samples	Well Water Volume (mL)	Volume of 0.01 M NaOH added (µL)	Volume of 5 ppm CN (in 0.01 M NaOH) added (µL)
Blank	9	1000	0
0.01 ppm CN	9	980	20
0.05 ppm CN	9	900	100
0.1 ppm CN	9	800	200
0.5 ppm CN	9	0	1000

Samples	Measured ABS at 409nm	dA	d ε	b	dC
Blank	0.4169				
0.01 ppm CN	0.4042	0.0127	105500	0.1	1.20E-06
0.05 ppm CN	0.3962	0.0207	105500	0.1	1.96E-06
0.1 ppm CN	0.3831	0.0338	105500	0.1	3.20E-06
0.5 ppm CN	0.2957	0.1212	105500	0.1	1.15E-05

In the next experiment a series of cyanide standards were made so that when 10 µL were added to 2 ml of 9.2 µM Mb(III)H_2O in a 1 cm cuvette would equal 0.01, 0.05, 0.1 and 0.2 ppm cyanide and would have the same concentration of NaOH added. The initial cyanide standards were prepared in 0.01 M NaOH. Approximately 0.5 minutes into the absorbance scan at 409 nm a 10 µL spike of the cyanide standard was added to give the desired ppm cyanide concentration. In this experiment the solution was not vortex mixed or stirred as in the previous experiments, and the cyanide was allowed to diffuse through the sample and bind to Mb(III)H_2O. Each reaction was allowed to proceed for 25 minutes (FIGURE 12a). The absorbance was averaged from 24.5 to 25 minutes and then subtracted from the initial averaged absorbance from 0 to 0.5 min and plotted as the Mb(III)H_2O concentration change versus cyanide concentration (FIGURE 12b).

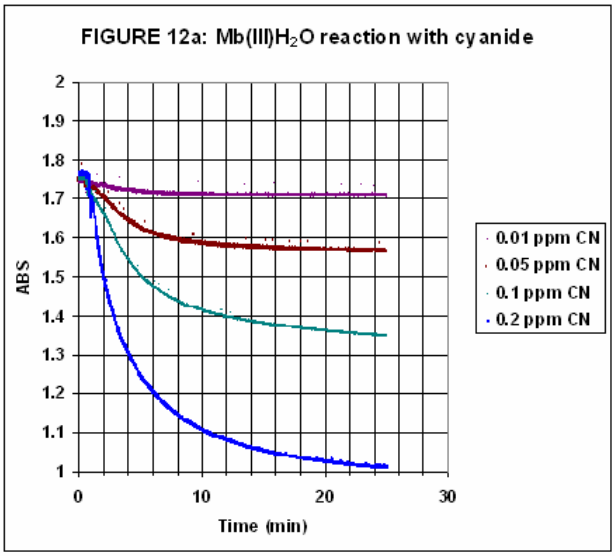

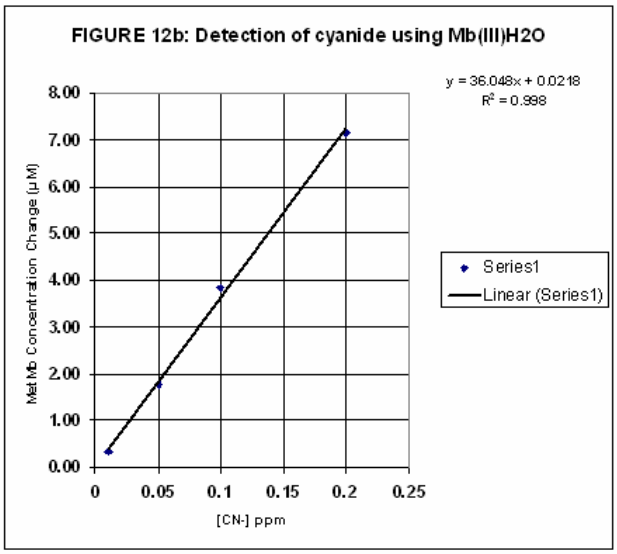

Samples	dA	d ε	b	dC
0.01 ppm CN	0.0354	105500	1	3.353E-07
0.05 ppm CN	0.1847	105500	1	1.751E-06
0.1 ppm CN	0.4037	105500	1	3.826E-06
0.5 ppm CN	0.7546	105500	1	7.152E-06

IV. Conclusions:

Two observations should be considered when preparing a CCO modified electrode on silver. First, the OM deposition is much faster and appears to be more predictable when the electrode is not characterized with cyclic voltammetry using phosphate buffer after the preparations steps. Second, using a double junction reference electrode for electrochemical measurements and not having KCl in the reference electrode during the bilayer formation will eliminate possible chloride interference. There may be extremely small pinholes or cracks in the reference electrode that are not visible to the eye, which is probably the reason the silver chloride peaks were so large. These cracks or pinholes may form during the preparation of the reference electrode when heating the glass to seal around the frit. In addition the reference electrode frit itself is porous and

will have a leak rate. However, single junction electrodes may be fine to use if the electrode frits have a small leak rate and the glass body is completely free of pinholes / cracks. Chloride interference may not be noticeable in these cases. Regardless of whether the reference electrode has a small leak rate or was made defect free, it is recommended that KCl be removed from the reference electrode when not in use and not placed in the reference electrode during bilayer formation.

Metmyoglobin may be used in the detection of cyanide. A molar absorptivity of 82500 M^{-1} cm^{-1} at 409 nm was found for $Mb(III)CN^-$ in the sample matrices analyzed. Cyanide samples may be preserved to a pH of 12. As long as the amount of preserved cyanide sample added to $Mb(III)H_2O$ does not raise the $Mb(III)H_2O$ pH environment much greater than 9.3 there is not much change in the absorbance. If other ligands present prove problematic in the direct determination the use of microdiffusion cells should help eliminate these interferences. This method may also be applicable to detection of cyanide in biological fluids if cyanide is liberated and captured in a microdiffusion cell containing $Mb(III)H_2O$.[80-82]

This research holds the potential for incorporating other membrane bound enzymes and exploiting their natural selectivity to toxic substances and their metabolites. Examples include the human liver cytochrome P450 and acetylcholinesterases, and information obtained with this research will be beneficial to these future objectives.

V. References:

1. Burgess, J. D.; Hawkridge, F. M., Octadecyl Mercaptan sub-monolayers on silver electrodeposited on gold quartz crystal microbalance electrodes. *Langmuir* **1997,** 13, 3781-3786.
2. Burgess, J. D.; Jones, V. W.; Porter, M. D.; Rhoten, M. C.; Hawkridge, F. M., Scanning force microscopy images of Cytochrome c Oxidase immobilized in an electrode-supported lipid bilayer membrane. *Langmuir* **1998,** 14, 6628-6631.
3. Burgess, J. D.; Rhoten, M. C.; Hawkridge, F. M., Cytochrome c Oxidase immobilized in stable supported lipid bilayer membranes. *Langmuir* **1998,** 14, 2467-2475.
4. Burgess, J. D.; Rhoten, M. C.; Hawkridge, F. M., Interconversion between resting and pulsed Cytochrome c Oxidase in electrode-supported lipid bilayer membranes. *J. Am. Chem. Soc.* **1998,** 120, 4488-4491.
5. Cullison, J. K.; Hawkridge, F. M.; Nakashima, N.; Yoshikawa, S., A study of Cytochrome c Oxidase in lipid bilayer membranes on electrode surfaces. *Langmuir* **1994,** 10, 877-882.
6. Rhoten, M. C.; Burgess, J. D.; Hawkridge, F. M., Temperature and pH effects on Cytochrome c Oxidase immobilized in an electrode-supported lipid bilayer membrane. *Electrochim. Acta* **2000,** 45, 2855-2860.
7. Rhoten, M. C.; Hawkridge, F. M.; Wilczek, J., The reaction of cytochrome c with bovine and Bacillus stearothermophilus Cytochrome c Oxidase immobilized in electrode supported lipid bilayer membranes. *J. Electroanal. Chem.* **2002,** 535, 97-106.
8. Su, L.; Kelly, J. B.; Hawkridge, F. M.; Rhoten, M. C.; Baskin, S. I., Characterization of cyanide binding to Cytochrome c Oxidase immobilized in electrode-supported lipid bilayer membranes. *J. Electroanal. Chem.* **2005,** 581, 241-248.
9. Baskin, S. I.; Brewer, T. G., *Chapter 10 - Cyanide poisoning*. Borden Institute: Washington D.C., **1997**; p 271-286.
10. Giovanni, F. M.; Sarti, P.; Brunori, M., Structure and function of a molecular machine: Cytochrome c Oxidase. *Biophys. Chem.* **1995,** 54, 1-33.
11. Capaldi, R. A., Structure and function of Cytochrome c Oxidase. *Annu. Rev. Biochem.* **1990,** 59, 569-596.
12. Hill, B. C., The reaction of electrostatic cytochrome c -Cytochrome c Oxidase complex with oxygen. *J. Biol. Chem.* **1991,** 266, 2219-2226.
13. Hill, B. C., Modeling the sequence of electron transfer reactions in the single turnover of reduced, mammalian Cytochrome c Oxidase with oxygen. *J. Biol. Chem.* **1992,** 269, 2419-2425.
14. Ferguson-Miller, S.; Babcock, G. T., Heme/copper terminal oxidases. *Chem. Rev.* **1996,** 96, 2889-2907.
15. Blomberg, M. R. A.; Siegbahn, P. E. M.; Babcock, G. T.; Wikstrom, M., O-O bond splitting mechanism in cytochrome oxidase. *J. Inorg. Biochem.* **2000,** 80, 261-269.
16. Einarsdottir, O., Fast reactions of Cytochrome Oxidase. *Biochim. Biophys. Acta* **1995,** 1229, 129-147.
17. Einarsdottir, O.; Szundi, I., Time-resolved optical absorption studies of cytochrome oxidase dynamics. *Biochim. Biophys. Acta* **2004,** 1655, 263-273.

18. Szundi, I.; Eps, N. V.; Einarsdottir, O., pH dependence of the reduction of dioxygen to water by Cytochrome c Oxidase. 2. branched electron transfer pathways linked by proton transfer. *Biochemistry* **2003,** 42, 5074-5090.
19. Baskin, S. I.; Petrikovics, I.; Kurche, J. S.; Nicholson, J. D.; Logue, B. A.; Maliner, B. I.; Rockwood, G. A., *Chapter 9 - Insights on cyanide toxicity and methods of treatment*. Narosa publishing house: **2004**; p 105-145.
20. Baskin, S. I.; Kurche, J. S.; Maliner, B. I., *Chapter 19 - Cyanide*. Humana press: **2003**; p 263-277.
21. Baker, G. M.; Noguchi, M.; Palmer, G., The reaction of Cytochrome c Oxidase with cyanide. *J. Biol. Chem.* **1987,** 262, 595-604.
22. VanBuuren, K. J. H.; Nicholls, P.; VanGelder, B. F., Biochemical and biophysical studies on cytochrome aa_3. VI. Reaction of cyanide with oxidized and reduced enzyme. *Biochim. Biophys. Acta* **1972,** 256, 258-276.
23. Das, T. K.; Mazumdar, S., Redox-linked conformational changes in bovine heart Cytochrome c Oxidase: Picosecond time-resolved fluorescence studies of cyanide complex. *Biopolymers (Biospectroscopy)* **2000,** 57, 316-322.
24. Pinakoulaki, E.; Vamvouka, M.; Varotsis, C., The active site structure of heme a_3^{3+} - $C\equiv N\text{-}Cu_B^{2+}$ of Cytochrome aa_3 Oxidase as revealed from resonanace raman scattering. *J. Phys. Chem. B.* **2003,** 107, 9865-9868.
25. Thomson, A. J.; Johnson, M. K.; Greenwood, C.; Gooding, P. E., A study of the magnetic properties of heme a3 in Cytochrome c Oxidase by using magnetic-circular-dichroism spectroscopy. *Biochem. J.* **1981,** 193, 687-697.
26. Tsubaki, M.; Yoshikawa, S., Fourier-transform infrared study of cyanide binding to the $Fe_{a3}\text{-}Cu_b$ binuclear site of bovine heart Cytochrome c Oxidase: implication of the redox-linked conformational change at the binuclear site. *Biochemistry* **1993,** 32, 164-173.
27. Yoshikawa, S.; Mochizuki, M.; Zhao, X. J.; Caughey, W. S., Effects of overall oxidation state on infrared spectra of Heme a_3 cyanide in bovine heart Cytochrome c Oxidase. *J. Biol. Chem.* **1995,** 270, 4270-4279.
28. Johnson, M. K.; Eglinton, D. G.; Goodig, P. E.; Greenwood, C.; Thomson, A. J., Characterization of the partially reduced cyanide-inhibited derivative of Cytochrome c Oxidase by optical, electron-paramagnetic-resonance and magnetic-circular-dichroism spectroscopy. *Biochem. J.* **1981,** 193, 699-708.
29. Nagasawa, H. T.; Cummings, S. E.; Baskin, S. I., The structure of "ITCA," a urinary metabolite of cyanide. *OPPI* **2004,** 36, 178-182.
30. Bitner, S.; Kanthasamy, A.; Isom, G. E.; Yim, G. K. W., Seizures and selective CA-1 hippocampal lesions induced by an excitotoxic cyanide metabolite, 2-iminothiazolidine-4-carboxylic acid. *NeuroToxicology* **1995,** 16, 115-122.
31. Marrs, T., Antidotal treatment of acute cyanide poisoning. *Adverse Drug React. Acute Poisoning Rev.* **1988,** 4, 179-206.
32. Al-Qarawi, A. A.; Mousa, H. M.; Ali, B. H., Tissue and intracellular distribution of rhodanese and mercaptopyruvate sulphurtransferase in ruminants and birds. *Vet. res.* **2001,** 32, 63-70.
33. Saidu, Y., Physicochemical features of rhodanese: A review. *African Journal of Biotechnology* **2004,** 3, 370-374.
34. Westley, J.; Adler, A.; Westley, L.; Nishida, C., The sulfur transferases. *Fund. and Appl. Toxicol.* **1983,** 3, 377-382.

35. Isom, G. E.; Burrows, G. E.; Way, J. L., Effect of oxygen on the antagonism of cyanide intoxication-cytochrome oxidase. *Toxicol. Appl. Pharmacol.* **1982,** 65, 250-256.
36. Isom, G. E.; Way, J. L., Lethality of cyanide in the absence of inhibition of liver cytochrome oxidase. *Biochem. Pharmacol.* **1976,** 25, 605-608.
37. Way, J. L., Cyanide prophylaxis and cytochrome c oxidase. *Defense Technical Information Center* **1985,** AD-A176-358.
38. Albaum, H. G.; Tepperman, J.; Bodansky, O., The in vivo inactivation by cyanide on brain cytochrome oxidase and its effect on glycolysis and on the high energy phosphorus compounds in the brain. *J. Biol. Chem.* **1946,** 164, 45-51.
39. Albaum, H. G.; Tepperman, J.; Bodansky, O., A spectrophotometric study of the competition of methemoglobin and cytochrome oxidase for cyanide *in vitro*. *J. Biol. Chem.* **1946,** 163, 641-647.
40. Tarkowski, S., Effect of cobalt on the inhibition of the cytochrome oxidase activity by potassium cyanide. *Med. Pracy.* **1966,** 17, 116-119.
41. Bartelheimer, E. W.; Friedberg, K. D.; Lendie, L., The potentialities of cobalt compounds for chemical reactions in relation to their toxicity and antidotal activity against hydrocyanic acid. *Archs. int. Pharmacodyn.* **1962,** 139, 99-108.
42. Evans, C. L., Cobalt compounds as antidotes for hydrocyanic acid. *Brit. J. Pharmac. Chemother.* **1964,** 23, 455-475.
43. Friedberg, K. D.; Shukla, U. R., The efficiency of aquocobalamin as an antidote in cyanide posioning when given alone or combined with sodium thiosulfate. *Arch. Toxicol.* **1975,** 33, 103-113.
44. Halpern, J.; Guastalla, G.; Bercaw, J., Some aspects of the chemistry of cobalt (I) cyanide and related complexes. *Coord. Chem. Rev.* **1972,** 8, 167-184.
45. Mshett, C. W.; Kelley, K. L.; Boxer, G. E.; Rickards, J. C., Efficacy of vitamin B12 (Hydroxo-cobalamin) in experimental cyanide poisoning. *Proc. Soc. Exp. Biol. Med.* **1952,** 81, 234-237.
46. Nagler, J.; Provcust, R. A.; Parizel, G., Hydrogen cyanide poisoning: treatment with cobalt. EDTA. *J. Occ. Med.* **1978,** 20, 414-416.
47. Paulet, G., Intoxication cyanhydrique et chelates de cobalt. *J. Physiol.* **1958,** 50, 438-542.
48. Rose, C. L.; Worth, R. M.; Chen, K. K., Hydroxocobalamine and acute cyanide poisoning in dogs. *Life Sci.* **1965,** 4, 1785-1789.
49. Way, J. L., Cyanide intoxication and its mechanism of antagonism. *Annu. Rev. Pharmacol. Toxicol.* **1984,** 24, 451-481.
50. Bryant, M. A.; Pemberton, E., Surface Raman scattering of self-assembled monolayers formed from 1-alkanethiols: Behavior of films at Au and comparison to films at Ag. *J. Amer. Chem. Soc.,* **1991,** 113, 8284-8293.
51. Sellers, H.; Ulman, A.; Shnidman, Y.; Eilers, J. E., Structure and binding of alkanethiolates on gold and silver surfaces: Implications for self-assembled monolayers. *J. Amer. Chem. Soc.* **1993,** 115, 12391-12397.
52. Soulimane, T.; Buse, G., Integral Cytochrome c Oxidase: Preparation and progress towards a three dimensional crystallization. *Eur. J. Biochem.* **1995,** 227, 588-595.
53. Hinkle, P. C.; Kim, J. J.; Racker, E., Ion transport and respiratory control in vesicles formed from cytochrome oxidase and phospholipids. *J. Biol. Chem.* **1972,** 247, 1338.
54. Awasthi, Y. C.; Chuang, T. F.; Keenan, T. W.; Crane, F. L., Tightly bound cardiolipin in Cytochrome c Oxidase. *Biochim. Biophys. Acta* **1971,** 226, 42-52.

55. Robinson, N. C., Specificity and binding affinity of phospholipids to the high affinity cardiolipin sites of beef heart cytochrome c oxidase. *Biochemistry* **1982,** 21, 184-188.
56. Robinson, N. C.; Capaldi, R. A., Interaction of detergents with Cyotchrome c Oxidase. *Biochemistry* **1977,** 16, 375-381.
57. Robinson, N. C.; Strey, F.; Talbert, L., Investigation of the essential boundary layer phospholipids of Cytochrome c Oxidase using Triton X-100 delipidation. *Biochemistry* **1980,** 19, 3656-3661.
58. Vik, S. B.; Capaldi, R. A., Lipid requirements for Cytochrome c Oxidase activity. *Biochemistry* **1977,** 16, 5755-5759.
59. Tsukihara, T.; Aoyama, H.; Yamashita, E.; Tomizaki, T.; Yamaguchi, H.; Shinzawa-Itoh, K.; Nakashima, R.; Yaono, R.; Yoshikawa, S., Structure of metal sites of oxidized bovine heart Cytochrome c Oxidase at 2.8 Å resolution. *Science* **1995,** 269, 1069-1074.
60. Tsukihara, T.; Aoyama, H.; Yamashita, E.; Tomizaki, T.; Yamaguchi, H.; Shinzawa-Itoh, K.; Nakashima, R.; Yaono, R.; Yoshikawa, S., The whole structure of the 13 subunit oxidized Cytochrome c Oxidase at 2.8 Å. *Science* **1996,** 272, 1136-1144.
61. Kadenbach, B.; Jarausch, J.; Hartmann, R.; Merle, P., Separation of mammalian Cytochrome c oxidase into 13 polypeptides by a sodium dodecyl sulfate-gel electrophoretic procedure. *Anal. Biochem.* **1983,** 129, 517-521.
62. Tsukihara, T.; Shimokata, K.; Katayama, Y.; Shimada, H.; Muramoto, K.; Aoyama, H.; Mochizuki, M.; Shinzawa-Itoh, K.; Yamashita, E.; Yao, M.; Ishimura, Y.; Yoshikawa, S., The low-spin heme of Cytochrome c Oxidase as the driving element of the proton-pumping process. *Proc. Natl. Acad. Sci. USA* **2003,** 100, 15304-15309.
63. Tsukihara, T.; Yoshikawa, S., Crystal structural studies of a membrane protein complex, Cytochrome c oxidase from bovine heart. *Acta Cryst.* **1998,** A54, 885-904.
64. Azzi, A., Cytochrome c Oxidase - Towards a clarification of its structure, interactions and mechanism. *Biochim. Biophys. Acta* **1980,** 594, 231-252.
65. Frey, T. G.; Chan, S. H. P.; Schatz, G., Structure and orientation of Cytochrome c Oxidase in crystalline membranes. *J. Biol. Chem.* **1978,** 253, 4389-4395.
66. Frey, T. G.; Murray, J. M., Electron microscopy of Cytochrome c Oxidase crystals - monomer-dimer relationship and cytochrome c binding site. *J. Mol. Biol.* **1994,** 237, 275-297.
67. Henderson, R.; Capaldi, R. A.; Leigh, J. S., Arrangement of Cytochrome c Oxidase molecules in two-dimensional vesicle crystals. *J. Mol. Biol.* **1977,** 112, 631-648.
68. Wittenberg, B. A.; Wittenberg, J. B., Myoglobin-mediated oxygen delivery to mitochondria of isolated cardiac myocytes. *Proc. Natl. Acad. Sci. USA* **1987,** 84, 7503-7507.
69. Edmundson, A. B.; Hirs, C. H. W., *J. Mol. Biol.* **1962,** 5, 663-682.
70. Wittenberg, B. A.; Wittenberg, J. B., Role of Myoglobin in the Oxygen Supply to Red Skeletal Muscle. *J. Biol. Chem.* **1975,** 250, 9038-9043.
71. King, B. C.; Hawkridge, F. M.; Hoffman, B. M., Electrochemical studies of cyanometmyoglobin and metmyoglobin: Implications for long-range electron transfer in proteins. *J. Am. Chem. Soc.* **1992,** 114, 10603-10608.
72. Sander, R., Compilation of Henry's Law Constants for Inorganic and Organic Species of Potential Importance in Environmental Chemistry (Version 3). *http://www.mpch-mainz.mpg.de/~sander/res/henry.html* **1999**.

73. Bates, R. G., Determination of pH: Theory and Practice. In John Wiley & Sons New York, **1985**; p 299.
74. Bruckenstein, S.; Shay, M., Experimental aspects of use of the quartz crystal microbalance in solution. *Electrochim. Acta* **1985,** 30, 1295-1300.
75. Sauerbrey, G., The use of quartz oscillators for weighing thin layers and for microweighing. *Phys. Z.* **1959,** 155, 206-222.
76. Gelder, B. F. V.; Slater, E. C., The extinction coefficient of cytochrome c. *Biochim. Biophys. Acta* **1962,** 58, 593-595.
77. Margoliash, E.; Schejter, A., Cytochrome c. *Adv. Protein Chem.* **1966,** 21, 113-286.
78. Anontini, E.; Brunori, M., Hemoglobin and Myoglobin in their reactions with ligands. In *Frontiers of Biology*, North-Holland: Amsterdam, **1971**; Vol. 21.
79. Bruckenstein, S.; Michaliski, M.; Fensore, A.; Li, Z.; A.R. Hillman, Dual quartz crystal microbalance oscillator circuit. Minimizing effects due to liquid viscosity, density, and temperature. *Anal. Chem.* **1994,** 66, 1847-1852.
80. Tomoda, A.; Hashimoto, K., The determination of cyanide in water and biological tissues by methemoglobin. *Journal of Hazardous Materials* **1991,** 28, 241-249.
81. Laforge, M.; Buneaux, F.; Houeto, P.; Bourgeois, F.; Bourdon, R.; Levillain, P., A rapid spectrophotometric blood cyanide determination applicable to emergency toxicology. *Journal of Analytical Toxicology* **1994,** 18, 173-175.
82. Holzbecher, M.; Ellenberger, H. A., An evaluation and modification of a microdiffusion method for the emergency determination of blood cyanide. *Journal of Analytical Toxicology* **1985,** 9, 251-253.

Appendix A: Analytical Equipment Obtained

1. CH Instruments Electrochemical Workstation (Austin, TX)
2. Varian Cary 50 Spectrophotometer (Palo Alto, CA)
3. Metrohm Ion Chromatography System (Houston, TX)
4. Millipore Ultrapure Water System (Billerica, MA)
5. Yamato PID controlled forced air convection oven (South San Francisco, CA)
6. Harvard Syringe Pumps (Holliston, MA)
7. Novascan UV/ozone surface cleaner (Ames, IA)
8. Dell Computer (Austin, TX)
9. Ultrasonic Cleaner (Danbury, CT)
10. Thermo electron Magna 560 MidIR spectrometer (Waltham, MA)
11. Remspec Mid-IR fiber optic probe (Charlton, MA)
12. Ocean Optics Fluorometer with oxygen sensing probe (Dunedin, FL)

Appendix B. Reference Oscillator Specifications

FOX

5.0V TTL CLOCK OSCILLATOR
MODEL: F1100E

FEATURES
- 5.0V Operation
- TTL Output
- 14-Pin DIP

FASTFOX Quote it!

• PART NUMBER SELECTION Learn More - Internet Required

Part Number	Model Number	Frequency Stability[1]	Operating Temperature (°C)	Frequency Range (MHz)
049-Frequency-xxxxx	F1100E	±100PPM(STD)	0 ~ +70	1.000 ~ 100.000
343-Frequency-xxxxx	F1100ER	±100PPM	-40 ~ +85	1.000 ~ 100.000
060-Frequency-xxxxx	F1145E	±50PPM	0 ~ +70	1.000 ~ 100.000
061-Frequency-xxxxx	F1145ER	±50PPM	-40 ~ +85	1.000 ~ 70.000
055-Frequency-xxxxx	F1144E	±25PPM	0 ~ +70	1.000 ~ 100.000
465-Frequency-xxxxx	F1144ER	±25PPM	-40 ~ +85	1.000 ~ 70.000

• ELECTRICAL CHARACTERISTICS

PARAMETERS	MAX (unless otherwise noted)
Frequency Range (Fo)	1.000 ~ 100.000 MHz
Storage Temperature Range (Tstg)	-55°C ~ +125°C
Supply Voltage (Vdd)	5.0V ± 10%
Input Current (Idd)	
1.000 ~ 8.000 MHz	15mA
8.000+ ~ 24.000 MHz	30mA
24.000+ ~ 70.000 MHz	70mA
70.000+ ~ 100.000 MHz	80mA
Output Symmetry (1.4V Level)	
1.000 ~ 8.000 MHz	45% ~ 55%
8.000+ ~ 100.000 MHz	40% ~ 60%
Rise Time (0.5V ~ 2.4V) (Tr)	
1.000 ~ 25.000 MHz	10 nS
25.000+ ~ 70.000 MHz	5 nS
70.000+ ~ 100.000 MHz	4 nS
Fall Time (2.4V ~ 0.5V) (Tf)	
1.000 ~ 25.000 MHz	10 nS
25.000+ ~ 70.000 MHz	5 nS
70.000+ ~ 100.000 MHz	4 nS
Output Voltage	
1.000 ~ 25.000 MHz (Vol)	0.4V
25.000+ ~ 100.000 MHz	0.5V
1.000 ~ 100.000 MHz (Voh)	2.4V Min
Output Current (Iol)	20mA Min
(Ioh)	-1.0mA Min
Output Load	10TTL
Start-up Time (Ts)	
1.000 ~ 3.500 MHz	20mS
3.500+ ~ 4.000 MHz	35mS
4.000+ ~ 6.000 MHz	30mS
6.000+ ~ 20.000 MHz	20mS
20.000+ ~ 100.000 MHz	15mS

[1] Inclusive of 25°C tolerance, operating temperature range, input voltage change, load change, aging, shock, and vibration.

All specifications subject to change without notice. *Rev. 6/1/04*

Learn more about:
Part Marking Identification
Mechanical Specification
Internet required

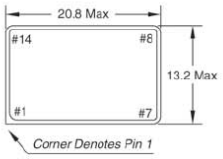

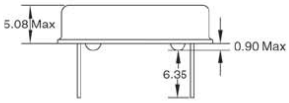

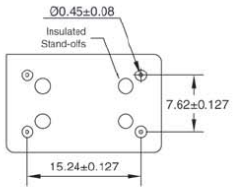

Pin Connections

#1 N.C. #8 Output
#7 GND (Case) #14 +5Vdc

All dimensions are in millimeters.

68 FOX Electronics 5570 Enterprise Parkway Fort Myers, Florida 33905 USA +1(239)693-0099 FAX +1(239)693-1554 http://www.foxonline.com

FULL SIZE 14 PIN DIP
Pin Connections
#1 N.C. #8 Output
#7 GND #14 VDD

Package A

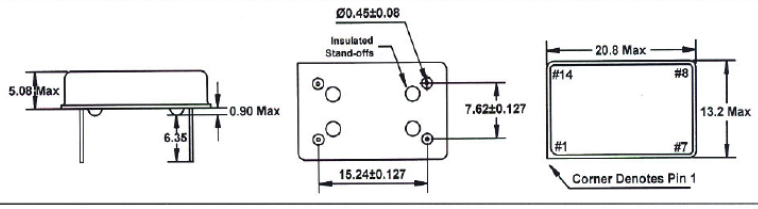

JITO®-2 Specifications

ELECTRICAL CHARACTERISTICS (CL = Max Load; HCMOS Option = Single Output)

PARAMETERS	FREQUENCY RANGE	CONDITIONS	MIN	MAX	UNITS
Frequency Range (Fo)			0.340	250.000	MHZ
Frequency Stability	0.340 ~ 250.000	All Conditions[1]	-100 -50 -30 -25 -20	+100 +50 +30 +25 +20[3]	PPM
Temperature Range Operating (TOPR) Storage (TSTG)	0.340 ~ 250.000		-20 -40 -55	+70 +85 +125	°C
Supply Voltage (VDD)	0.340 ~ 250.000		+4.5 +3.0	+5.5 +3.6	V
Input Current**	0.340 ~ 25.000 25.000+ ~ 50.000 50.000+ ~ 150.000 150.000+ ~ 250.000	VDD = 5.0V Max Load (HCMOS)		15 20 33 55	mA
	0.340 ~ 200.000[4]	VDD = 5.0V PECL		55	
	0.340 ~ 25.000 25.000+ ~ 50.000 50.000+ ~ 150.000 150.000+ ~ 250.000	VDD = 3.3V Max Load (HCMOS)		8 11 21 30	
	0.340 ~ 200.000[4]	VDD = 3.3V PECL		30	
Output Symmetry	0.340 ~ 250.000	50% VDD Level HCMOS	45	55	%
	0.340 ~ 200.000[4]	50% Vp-p Level PECL	40	60	
Rise Time	0.340 ~ 250.000	10% ~ 90% VDD Level HCMOS		5	nS
	0.340 ~ 200.000[4]	20% ~ 80% Vp-p Level PECL		2	
Fall Time	0.340 ~ 250.000	90% ~ 10% VDD Level HCMOS		5	
	0.340 ~ 200.000[4]	80% ~ 20% Vp-p Level PECL		2	
Output Voltage HCMOS (VOL) (VOH)	0.340 ~ 250.000	VDD = 5.0V±10% IOL = 4mA IOH = -4mA	90%VDD	10%VDD	V
(VOL) (VOH)		VDD = 3.3V±10% IOL = 2mA IOH = -2mA	90%VDD	10%VDD	
PECL (VOL) (VOH)	0.340 ~ 200.000[4]	VDD = 5.0V Per recommended termination	3.0 3.9	3.4 4.3	V
(VOL) (VOH)		VDD = 3.3V Per recommended termination	1.2 2.2	1.6 2.6	
Output Current HCMOS (IOL) (IOH)	0.340 ~ 250.000	VDD = 5.0V±10% VOL = 10%VDD VOH = 90% VDD		4 -4	mA
(IOL) (IOH)		VDD = 3.3V±10% VOL = 10%VDD VOH = 90%VDD		2 -2	
Output Load	0.340 ~ 100.000 100.000+ ~ 250.000	VDD = 5.0V±10% (HCMOS)		25 10	pF
	0.340 ~ 100.000 100.000+ ~ 250.000	VDD = 3.3V ±10% (HCMOS)		15 10	
Start-up Time (Ts)	0.340 ~ 250.000			10	mS
Enable/Disable Time[2] (JITO®-2 D) (JITO®-2 P)	0.340 ~ 250.000			100	nS
Output Skew (JITO®-2 D) (PECL)	0.340 ~ 200.000[4]	50% Vp-p		500	pS

[1] Inclusive of 25°C tolerance, operating temperature range, input voltage change, load change, aging, shock and vibration.
[2] Stand by current (3.3V) = 60µA (MAX) • Stand by enable time = 10mS (MAX)
[3] Inclusive of 25°C tolerance, operating temperature range, input voltage change, load change, shock and vibration.
[4] PECL can be programmed to 250 MHz; output terminations may have to be modified for desired output levels. See Application Note "JITO-2 PECL Interface Considerations".

NOTE: A0.01µF bypass capacitor should be placed between VDD and GND to minimize power supply line noise.

ENABLE/DISABLE FUNCTION	
PIN 1	Output MIN-6: Pins 4&2 (PECL) JITO®-2 P: Pin 3
OPEN	ACTIVE
'1' Level VIH ≥ 70%VDD	ACTIVE
'0' Level VIL ≤ 30%VDD	High Z

JITO®-2
JUST-IN-TIME OSCILLATORS®

Covered by U.S. Patents 5,952,890 and 5,960,405 and 6,188,290. Covered by one or more listed Foreign Patents: R.S.A. 98/0866 and R.O.C. 120851.

JITO®-2 . Only from Fox Electronics. Because in this business, timing is everything.